MHD flow and heat transfer over a porous oscillating stretching surface in a viscoelastic fluid

By

Sami Ullah Khan

A Thesis
Submitted in the Partial Fulfillment of the
Requirements for the Degree of
MASTER OF SCIENCE
In
MATHEMATICS

Supervised by

Dr. Zaheer Abbas

Department of Mathematics & Statistics
Faculty of Basic and Applied Sciences
International Islamic University, Islamabad
Pakistan, 2011

1 - Flow ; fluid mechanics

2 - Fluid mechanics

In the name of almighty ALLAH,
the most beneficient, the most merciful

MHD flow and heat transfer over a porous oscillating stretching surface in a viscoelastic fluid

By

Sami Ullah Khan

Department of Mathematics & Statistics
Faculty of Basic and Applied Sciences
International Islamic University, Islamabad
Pakistan, 2011

MHD flow and heat transfer over a porous oscillating stretching surface in a viscoelastic fluid

By

Sami Ullah Khan

Supervised by

Dr. Zaheer Abbas

Department of Mathematics & Statistics
Faculty of Basic and Applied Sciences
International Islamic University, Islamabad
Pakistan, 2011

Certificate

MHD flow and heat transfer over a porous oscillating stretching surface in a viscoelastic fluid

By

Sami Ullah Khan

A DISSERTATION SUBMITTED IN THE PARTIAL FULFILLMENT OF THE REQUIREMENTS FOR THE DEGREE OF THE **MASTER OF SCIENCE IN MATHEMATICS**

We accept this dissertation as conforming to the required standard.

1. _____
Dr. Zaheer Abbas
(Supervisor)

2. _____
Dr. Ahmad Zeeshan
(Internal Examiner)

3. _____
Prof. Dr. Muhammad Ozair Ahmad
(External Examiner)

4. _____
Dr. Irshad Ahmad Arshad
(Chairman)

Department of Mathematics & Statistics
Faculty of Basic & Applied Science
International Islamic University Islamabad,
Pakistan, 2011.

Declaration

I, hereby declare that this dissertation, neither as a whole nor as a part thereof, has been copied out from any source. It is further that I have prepared this dissertation entirely on the basses of my personal effort made under the sincere guidance of my supervisor. No portion of the work, presented in this dissertation, has been submitted in support of any application of any degree or qualification of this or any other university or institute of learning.

Signature: _____

Sami Ullah Khan
MS (Mathematics)
Registration No: 34-FBAS/MSMA/F09
Department of Mathematics and Statistics Faculty of Basic and Applied Sciences International Islamic University, Islamabad, Pakistan.

Dedicated to

HOLY PROPHET HAZRAT MUHAMMAD (PBUH)

Acknowledgements

Foremost, I am always grateful to Almighty ALLAH, who made human being, the best creation of all the living species and made them understand to write with pen. He provided me the boldness and capability to achieve this task. I offer countless Darood and Salaams to my beloved Holy Prophet Hazrat Muhammad (PBUH), for whom this universe has been manifested. ALLAH has shown His existence and ones by sending him as a messenger of Islam and born me as a Muslim.

I offer my most sincere gratitude to my affectionate, sincere, kind and most respected supervisor Dr. Zaheer Abbas, **whose kinetic supervision, admonition in a right inclination and inductance of hard work made my task easy and I completed my dissertation well with in time. I am also grateful to my teachers Dr. Nasir Ali, Dr. Tariq Javed from whom I learned a lot. My sincere thanks also go to Dr. Ahmed Zeeshan.**

I would like to thanks my parents for supporting me emotionally and financially. I feel the completion of this dissertation as a grant of their prayers. Special thanks to my sister Sanam Junejo who has not only encouraged me but also supported financially throughout my life.

I also offer special thanks to all my friend Iftikhar Akhtar, and my class fellows Abuzr, Mudasar Raheel, Khurum, Asif who really helped me to their best throughout my research period. They helped me throughout my work, whenever I faced any difficulty relating my problem.

Date: December 13, 2011 **Sami Ullah Khan**

Preface

Many fluids in the industry and technology do not obey the Newton's law of viscosity and are usually classified as a non-Newtonian in nature. For example, blood, yoghurt, ketchup, shampoo, mud, paint, polymer melts and greases etc. have complicated relationship between the shear stress and rate of strain are non-Newtonian fluids. The boundary layer flow of these fluids and heat transfer analysis on a continuously moving surface has a wide range of application on engineering and industrial process, for example, the manufacture of plastic fluids, artificial fibers and polymeric sheets, plastic foam processing, in the extrusion of a polymer sheet from a die, heat treated materials travelling between a feed role and many others. After the work of Sakiadis [1,2] on a continuous moving surface, many researchers studied the various aspects of flow and heat transfer characteristics in a non-Newtonian fluid with/without magnetic field over a stretching surface. Some important studies are Rajagopal et al. [3], Dandapat and eqiptra [4], McLeod and Rajagopal [5], Rollins and Vajravelu [6, Cortell [7,8], Nazar et al. [9], Ishak et al. [10], Hayat et al. [11] and many references their in.

In the above mentioned investigations the stretching velocity of the sheet is linearly proportional to the distance along the flow. To the best of our knowledge, Wang [12] first discussed the various flow due to an oscillating stretching surface. The flow is induced due to an infinite elastic sheet which is stretched back and forth in its own plane. Abbas et al. [13] extended the problem of [12] to study the heat transfer of a viscous fluid over oscillatory stretching surface with flow/ thermal slip condition. Recently, Abbas et al. [13] attempted the firs problem regarding the boundary layer flow of a second grade fluid due to an oscillatory stretching sheet with magnetic field. They have also studied the non-linear partial differential equation both numerically using finite-difference method and analytically using homotopy analysis method (HAM). In the light of this, the present dissertation is arranged as follows:

Chapter one aim to present some basic definitions and flow equations which one used in fluid mechanics. Chapter two deals the boundary layer flow of an electrically conducting second grade fluid due to an oscillatory stretching surface. The solution of the non-linear partial differential equations obtained numerically by employing finite difference method. The influence of the interesting parameters on the velocity field and skin-friction coefficient is shown through graphs and tables. This chapter is a review of the work done by Abbas et al. [14].

Chapter three looks at the MHD flow and heat transfer over a porous oscillating stretching sheet in a viscoelastic fluid. The governing flow equations are transformed into a set of non-linear partial differential equations. The finite difference method is employed to obtain the solution of this system. The effects on the flow, temperature field, the skin-friction coefficient and the local Nusselt number are shown through graphs and tables. In fact, this chapter is an extension of the work done by Abbas et al. [14].

Contents

Chapter 1

Basic Definitions

This chapter aims to describes some basic definitions and flow equations which are used in fluid mechanics. The basic idea of finite difference method is also given in this chapter.

1.1 Fluid Mechanics

It is the branch of engineering and physics that deals with nature and properties of the fluid both in motion or at rest. In practice, the study of fluid mechanics can be divided into the categories.

1.2 Flow

Flow is a substance or material goes under deformation in the presence of different forces. If the deformation exceeds continuously without limit then this phenomenon is known as flow.

1.3 Fluid

A fluid is a substance or material that deforms continuously under the application of shear stress, no matter how is material small the shear stress.

1.4 Velocity Field

In dealing with fluid motion, we shall necessarily be concerned with the description of velocity field. In general at given instant the velocity field $\mathbf{V}$ is function of space coordinates x, y, z and time t. The velocity at any point in flow field might vary from one instant to another. The complete representation of velocity field is given

$$\mathbf{V} = \mathbf{V}(x,\ y,\ z,\ t). \tag{1.1}$$

1.5 Viscosity

In general, it is defined as the ratio of shear stress to rate of shear strain, i.e.

$$\mu = \frac{\text{shear stress}}{\text{rate of shear strain}} = \frac{\tau_{xy}}{(du/dy)}. \tag{1.2}$$

where μ is coefficient of viscosity.

1.6 Kinematic viscosity

It is the ratio of the viscosity to density of the fluid, and it is given as

$$\nu = \frac{\mu}{\rho}. \tag{1.3}$$

1.7 Classification of fluids

There are two main types of fluids

(i)Ideal fluids

(ii) Real fluids

(i) Ideal fluids

A fluid for which viscosity is zero are termed as ideal fluid. The fluids with zero viscosity offers no resistance to shearing forces and hence during the flow the deformation of fluid all shear forces are zero. An ideal fluid is fictitious and does not exist in nature however many

fluids under certain engineering applications show negligible viscosity effects and can be treated as ideal fluids.

(ii) Real fluids

All fluids for which the viscosity is not equal to zero is known as real fluids. Real fluids are further divided into two main classes.

(a). Newtonian fluid

(b). Non-Newtonian fluid

(a) Newtonian fluid

All fluids which satisfy the Newton's law of viscosity are called Newtonian fluids. The Newtonian law of viscosity is stated as "shear stress is directly and linearly proportional to rate of deformation". Mathematically, it is stated as

$$\tau_{yx} \propto \frac{du}{dy}, \tag{1.4}$$

or

$$\tau_{yx} = \mu \left(\frac{du}{dy} \right), \tag{1.5}$$

where τ_{yx} is the shear stress acting in the plane normal to y-axis and in the direction parallel to x-axis and μ is constant proportionality, known as absolute or dynamic viscosity. Water, air and gasoline are examples of Newtonian fluids.

(b) Non-Newtonian fluid

All fluids which do not obey Newton's law of viscosity are called non-Newtonian fluids. These types of fluid obey the power law model in which shear stress is directly but nonlinearly proportional to the rate of deformation. Mathematically,

$$\tau_{yx} \propto \left(\frac{du}{dy} \right)^n, \ \mathrm{n} \neq 1, \tag{1.6}$$

$$\tau_{yx} = k \left(\frac{du}{dy} \right)^n, \tag{1.7}$$

where n is called the flow behavior index and k is the consistency index. Examples of non-Newtonian fluids are shampoo, gel, blood etc.

1.8 Internal flow systems

All those where fluid flows through confined spaces, e.g., flow through pipes, pumping of blood through blood arteries and water in channels.

1.9 External flow system

All those where confining boundaries are at relatively larger or at infinite distances such as atmosphere through airplane and space vehicles travels.

1.10 Stress field

A field in which surface forces and body forces are incountered called stress field. A stress field is a region where the stress (surface forces and body forces)is defined at every point.

1.11 Surface force

The surface force include all the forces acting on boundary through direct contact. Since theses forces act only in short range, therefore these forces are also called short range forces.

1.12 Body force

The forces which do not require any physical contact with boundary and distributed over the whole volume of the fluid are known as body forces. Gravitational and electromagnetic forces are categorized as body forces. These are infect long rang forces.

1.13 Pressure

Pressure is the surface force that acts normal to the area under consideration. The force per unit area is called pressure. Let A is the surface area of fluid and F is magnitude of force acting normal to surface, then pressure P due to the force on unit area of this surface is defined as

$$p = \frac{F}{A}. \tag{1.8}$$

1.14 Maxwell's equations

Maxwell's equations are the set of four equations which relate the electric and magnetic field to their sources, charge density and current density. Individually, these equations are known as Guass's law, Gauss's law for magnetism, Faradays law of induction and Ampere's law with Maxxwells correction. These equations are described as

$$\nabla.\mathbf{E} = \frac{\rho}{\epsilon_0}, \tag{1.9}$$

$$\nabla.\mathbf{B} = 0, \tag{1.10}$$

$$\nabla \times \mathbf{E} = -\frac{\partial \mathbf{B}}{\partial t}, \tag{1.11}$$

$$\nabla \times \mathbf{B} = \mu_0 \mathbf{J} + \mu_0 \epsilon_0 \frac{\partial \mathbf{E}}{\partial t}. \tag{1.12}$$

In above equations ϵ_0 is the permittivity of the free space also called electric constant, μ_0 is the permeability of free space which is also called magnetic constant, ρ is the total charge density and $\mathbf{J}$ is the total current density. The total magnetic field is $\mathbf{B}_0 = (B_0 + \mathbf{b})$, where $\mathbf{b}$ is induced magnetic field. By Ohm's law in generalized form we have

$$\mathbf{J} = \sigma \left(\mathbf{E} + \mathbf{V} \times \mathbf{B} \right), \tag{1.13}$$

where σ is the electric conductivity of the fluid. In the present case there is no applied electric field, also the induced magnetic field is neglected due the assumption of flow magnetic Reynold number. Therefore, the Lorentz force in the direction of the flow becomes

$$(\mathbf{J} \times \mathbf{B}) = -\sigma B_0^2 \mathbf{V}, \tag{1.14}$$

where B_0 is the applied magnetic field and $\mathbf{V}$ is the velocity.

1.15 Governing Equations

1.15.1 Equation of continuity

The mathematical relation of conservation of mass for fluid is known as equation of continuity. It has the following form

$$\frac{\partial \rho}{\partial t} + \boldsymbol{\nabla}.(\rho \mathbf{V}) = 0, \tag{1.15}$$

and for incompressible fluid it reduces to

$$\boldsymbol{\nabla}.\mathbf{V} = 0. \tag{1.16}$$

1.15.2 Equation of motion

The motion of fluid is governed by law of conservation of momentum. The application of this law to an arbitrary control volume in flowing fluid yield the following equation commonly known an equation of motion.

$$\rho \frac{d\mathbf{V}}{dt} = -\nabla p + \text{div}\mathbf{T} + \rho \mathbf{b}. \tag{1.17}$$

In above equation $\mathbf{T}$ is Cauchy stress tensor and $\mathbf{b}$ is body force per unit mass.

1.15.3 Energy equation

Energy in a system may take on various forms (e.g. kinetic, potential, heat, light). Mathematical form of energy equation is described as

$$\rho c_p \frac{D\theta}{Dt} = \mathbf{T}.\mathbf{L} - \boldsymbol{\nabla}.\mathbf{q}, \tag{1.18}$$

in which

$$\mathbf{L} = \boldsymbol{\nabla}\mathbf{V}. \tag{1.19}$$

Energy equation also represent the 'Law of Conservation of Energy'.

1.16 Boundary layer equation in second grade fluid

The law of conservation of momentum is given by

$$\rho\frac{d\mathbf{V}}{dt} = \operatorname{div}\tau + \mathbf{J}\times\mathbf{B}, \tag{1.20}$$

where $\mathbf{B}$ is the magnetic field and is given by

$$\mathbf{B} = (0, B_0, 0)\,. \tag{1.21}$$

The Cauchy stress tenser T for second grade fluid is

$$\mathbf{T} = -p\mathbf{I}+\mathbf{F}, \tag{1.22}$$

where $\mathbf{F}$ is the extra stress tensor and is given by

$$\mathbf{F} = \mu\mathbf{A}_1 + \alpha_1\mathbf{A}_2 + \alpha_2\mathbf{A}_1^2 \tag{1.23}$$

where p is the pressure, $\mathbf{I}$ is identity tensor, and α_1 and α_2 are material module and $\mathbf{A_1}$ and $\mathbf{A_2}$ are the Rivilin-Ericksen tensors and given by

$$\mathbf{A}_1 = \mathbf{L} + \mathbf{L}^{\mathrm{T}}, \tag{1.24}$$

$$\mathbf{A}_2 = \frac{d\mathbf{A_1}}{dt} + \mathbf{A_1}\mathbf{L} + \mathbf{L}^{\mathrm{T}}\mathbf{A}_1, \tag{1.25}$$

where $\mathbf{L} = \operatorname{grad}\mathbf{V}$ and $\mathbf{L}^{\mathrm{T}} = (\operatorname{grad}\mathbf{V})^T$ and $\frac{d}{dt}$ is the material derivative.

For unsteady two-dimensional flow, we take the velocity field in the form

$$V = [u(x,y,t),\ v(x,y,t),\ 0], \tag{1.26}$$

and

$$L = \begin{bmatrix} \frac{\partial u}{\partial x} & \frac{\partial u}{\partial y} & 0 \\ \frac{\partial v}{\partial x} & \frac{\partial v}{\partial y} & 0 \\ 0 & 0 & 0 \end{bmatrix}, \tag{1.27}$$

$$\mathbf{L}^{\mathrm{T}} = \begin{bmatrix} \frac{\partial u}{\partial x} & \frac{\partial v}{\partial x} & 0 \\ \frac{\partial u}{\partial y} & \frac{\partial v}{\partial y} & 0 \\ 0 & 0 & 0 \end{bmatrix}, \tag{1.28}$$

$$\mathbf{A}_1 = \begin{bmatrix} 2\frac{\partial u}{\partial x} & \frac{\partial u}{\partial y} + \frac{\partial v}{\partial x} & 0 \\ \frac{\partial u}{\partial y} + \frac{\partial v}{\partial x} & 2\frac{\partial v}{\partial y} & 0 \\ 0 & 0 & 0 \end{bmatrix}, \tag{1.29}$$

$$A_1 L = \begin{bmatrix} 2\left(\frac{\partial u}{\partial x}\right)^2 + \left(\frac{\partial u}{\partial y} + \frac{\partial v}{\partial x}\right)\frac{\partial v}{\partial x} & 2\frac{\partial u}{\partial x}\frac{\partial u}{\partial y} + \left(\frac{\partial u}{\partial y} + \frac{\partial v}{\partial x}\right)\frac{\partial v}{\partial y} & 0 \\ \left(\frac{\partial u}{\partial y} + \frac{\partial v}{\partial x}\right)\frac{\partial u}{\partial x} + 2\frac{\partial v}{\partial x}\frac{\partial v}{\partial y} & \left(\frac{\partial u}{\partial y} + \frac{\partial v}{\partial x}\right)\frac{\partial u}{\partial y} + 2\left(\frac{\partial v}{\partial y}\right)^2 & 0 \\ 0 & 0 & 0 \end{bmatrix}$$

$$L^{\mathrm{T}} A = \begin{bmatrix} 2\left(\frac{\partial u}{\partial x}\right)^2 + \left(\frac{\partial u}{\partial y} + \frac{\partial v}{\partial x}\right)\frac{\partial v}{\partial x} & \left(\frac{\partial u}{\partial y} + \frac{\partial v}{\partial x}\right)\frac{\partial u}{\partial x} + 2\frac{\partial u}{\partial x}\frac{\partial v}{\partial y} & 0 \\ 2\frac{\partial u}{\partial x}\frac{\partial u}{\partial y} + \frac{\partial v}{\partial y}\left(\frac{\partial u}{\partial y} + \frac{\partial v}{\partial x}\right) & \frac{\partial u}{\partial y}\left(\frac{\partial u}{\partial y} + \frac{\partial v}{\partial x}\right) + 2\left(\frac{\partial v}{\partial y}\right)^2 & 0 \\ 0 & 0 & 0 \end{bmatrix}$$

$$\mathbf{A}_1^2 = \begin{bmatrix} 4\left(\frac{\partial u}{\partial x}\right)^2 + \left(\frac{\partial u}{\partial y} + \frac{\partial v}{\partial x}\right)^2 & 2\frac{\partial u}{\partial x}\frac{\partial u}{\partial y} + \frac{\partial u}{\partial x}\frac{\partial v}{\partial x} + 2\frac{\partial v}{\partial y}\frac{\partial u}{\partial y} + 2\frac{\partial v}{\partial x}\frac{\partial v}{\partial y} & 0 \\ 2\frac{\partial u}{\partial x}\frac{\partial u}{\partial y} + 2\frac{\partial u}{\partial x}\frac{\partial v}{\partial x} + 2\frac{\partial u}{\partial y}\frac{\partial v}{\partial y} + 2\frac{\partial v}{\partial x}\frac{\partial v}{\partial y} & 4\left(\frac{\partial v}{\partial y}\right)^2 + \left(\frac{\partial u}{\partial y} + \frac{\partial v}{\partial x}\right)^2 & 0 \\ 0 & 0 & 0 \end{bmatrix}, \tag{1.30}$$

Now Eq. (1.25) becomes

$$\mathbf{A_2} = \begin{bmatrix} 2\frac{\partial^2 u}{\partial t \partial x} + 2u\frac{\partial^2 u}{\partial x^2} + 2v\frac{\partial^2 u}{\partial y \partial x} \\ +4\left(\frac{\partial u}{\partial x}\right)^2 + 2\left(\frac{\partial v}{\partial x}\right)^2 + 2\frac{\partial u}{\partial y}\frac{\partial v}{\partial x} \\ \frac{\partial^2 u}{\partial t \partial y} + \frac{\partial^2 v}{\partial t \partial x} + u\frac{\partial^2 u}{\partial x \partial y} + u\frac{\partial^2 v}{\partial x^2} \\ +v\frac{\partial^2 u}{\partial y^2} + 3\frac{\partial v}{\partial x}\frac{\partial v}{\partial y} + 3\frac{\partial u}{\partial x}\frac{\partial u}{\partial y} \\ +\frac{\partial u}{\partial y}\frac{\partial v}{\partial y} + \frac{\partial u}{\partial x}\frac{\partial v}{\partial x} + v\frac{\partial^2 v}{\partial x \partial y} \\ 0 \end{bmatrix} \quad \begin{bmatrix} \frac{\partial^2 u}{\partial t \partial y} + \frac{\partial^2 v}{\partial t \partial x} + u\frac{\partial^2 u}{\partial x \partial y} + u\frac{\partial^2 v}{\partial x^2} \\ +v\frac{\partial^2 u}{\partial y^2} + 3\frac{\partial v}{\partial x}\frac{\partial v}{\partial y} + 3\frac{\partial u}{\partial x}\frac{\partial u}{\partial y} \\ +\frac{\partial u}{\partial y}\frac{\partial v}{\partial y} + \frac{\partial u}{\partial x}\frac{\partial v}{\partial x} + v\frac{\partial^2 v}{\partial x \partial y} \\ 2\frac{\partial^2 v}{\partial t \partial y} + 2v\frac{\partial^2 v}{\partial y^2} + 2u\frac{\partial^2 v}{\partial x \partial y} \\ +4\left(\frac{\partial v}{\partial y}\right)^2 + 2\left(\frac{\partial u}{\partial y}\right)^2 + 2\frac{\partial u}{\partial y}\frac{\partial v}{\partial x} \\ 0 \end{bmatrix} \quad \begin{bmatrix} 0 \\ 0 \\ 0 \end{bmatrix} \tag{1.31}$$

After using the values of A_1, A_2 and A_1^2, Eq. (1.23) gives

$$\mathbf{F} = \begin{bmatrix} 2\mu\frac{\partial u}{\partial x} + \alpha_1\{2\frac{\partial^2 u}{\partial t\partial x} & \mu\left(\frac{\partial u}{\partial y} + \frac{\partial v}{\partial x}\right) + \alpha_1\{\frac{\partial^2 u}{\partial t\partial y} + \frac{\partial^2 v}{\partial t\partial x} & \\ +2u\frac{\partial^2 u}{\partial x^2} + 2v\frac{\partial^2 u}{\partial y\partial x} & +u\frac{\partial^2 u}{\partial x\partial y} + u\frac{\partial^2 v}{\partial x^2} + v\frac{\partial^2 u}{\partial y^2} + 3\frac{\partial v}{\partial x}\frac{\partial v}{\partial y} & \\ +4\left(\frac{\partial u}{\partial x}\right)^2 + 2(\frac{\partial v}{\partial x})^2 & +3\frac{\partial u}{\partial x}\frac{\partial u}{\partial y} + \frac{\partial u}{\partial y}\frac{\partial u}{\partial y} + \frac{\partial u}{\partial x}\frac{\partial v}{\partial x} + v\frac{\partial^2 v}{\partial x\partial y}\} & 0 \\ +2\frac{\partial u}{\partial y}\frac{\partial v}{\partial x}\} & +\alpha_2\left(2\frac{\partial u}{\partial x}\frac{\partial u}{\partial y} + \frac{\partial u}{\partial x}\frac{\partial v}{\partial x} + 2\frac{\partial v}{\partial y}\frac{\partial u}{\partial y} + 2\frac{\partial v}{\partial x}\frac{\partial v}{\partial y}\right) & \\ +\alpha_2\left[4\left(\frac{\partial u}{\partial x}\right)^2 + \left(\frac{\partial u}{\partial y} + \frac{\partial v}{\partial x}\right)^2\right] & & \\ \mu\left(\frac{\partial u}{\partial y} + \frac{\partial v}{\partial x}\right) + \alpha_1\{\frac{\partial^2 u}{\partial t\partial y} + \frac{\partial^2 v}{\partial t\partial x} & 2\mu\frac{\partial v}{\partial y} + \alpha_1\{2\frac{\partial^2 v}{\partial t\partial y} & \\ +u\frac{\partial^2 u}{\partial x\partial y} + u\frac{\partial^2 v}{\partial x^2} + v\frac{\partial^2 u}{\partial y^2} & +2v\frac{\partial^2 v}{\partial y^2} + 2u\frac{\partial^2 v}{\partial x\partial y} + 4\left(\frac{\partial v}{\partial y}\right)^2 & \\ +3\frac{\partial v}{\partial x}\frac{\partial v}{\partial y} + 3\frac{\partial u}{\partial x}\frac{\partial u}{\partial y} + \frac{\partial u}{\partial y}\frac{\partial v}{\partial y} & +2(\frac{\partial u}{\partial y})^2 + 2\frac{\partial u}{\partial y}\frac{\partial v}{\partial x}\} & 0 \\ +\frac{\partial u}{\partial x}\frac{\partial v}{\partial x} + v\frac{\partial^2 v}{\partial x\partial y}\} & +\alpha_2\left(4\left(\frac{\partial v}{\partial y}\right)^2 + \left(\frac{\partial u}{\partial y} + \frac{\partial v}{\partial x}\right)^2\right) & \\ +\alpha_2\left(2\frac{\partial u}{\partial x}\frac{\partial u}{\partial y} + 2\frac{\partial u}{\partial x}\frac{\partial v}{\partial x} + 2\frac{\partial u}{\partial y}\frac{\partial v}{\partial y} + 2\frac{\partial v}{\partial x}\frac{\partial v}{\partial y}\right) & & \\ 0 & 0 & 0 \end{bmatrix} \tag{1.32}$$

Using Eq.(1.32) in Eq.(1.22) gives

$$\begin{bmatrix} \tau_{xx} & \tau_{xy} & 0 \\ \tau_{yx} & \tau_{yy} & 0 \\ 0 & 0 & 0 \end{bmatrix} = \begin{bmatrix} -\frac{\partial p}{\partial x} & 0 & 0 \\ 0 & -\frac{\partial p}{\partial y} & 0 \\ 0 & 0 & 0 \end{bmatrix} \tag{1.33}$$

$$+ \begin{bmatrix} \begin{matrix} 2\mu\frac{\partial u}{\partial x} \\ +\alpha_1 \begin{bmatrix} 2\frac{\partial^2 u}{\partial t \partial x} + 2u\frac{\partial^2 u}{\partial x^2} \\ +2v\frac{\partial^2 u}{\partial y \partial x} + 4\left(\frac{\partial u}{\partial x}\right)^2 \\ +2(\frac{\partial v}{\partial x})^2 + 2\frac{\partial u}{\partial y}\frac{\partial v}{\partial x} \end{bmatrix} \\ +\alpha_2 \left[4\left(\frac{\partial u}{\partial x}\right)^2 + \left(\frac{\partial u}{\partial y} + \frac{\partial v}{\partial x}\right)^2\right] \end{matrix} & \begin{matrix} \mu\left(\frac{\partial u}{\partial y} + \frac{\partial v}{\partial x}\right) \\ +\alpha_1 \begin{bmatrix} \frac{\partial^2 u}{\partial t \partial y} + \frac{\partial^2 v}{\partial t \partial x} \\ +u\frac{\partial^2 u}{\partial x \partial y} + u\frac{\partial^2 v}{\partial x^2} \\ +v\frac{\partial^2 u}{\partial y^2} + 3\frac{\partial v}{\partial x}\frac{\partial v}{\partial y} \\ +3\frac{\partial u}{\partial x}\frac{\partial u}{\partial y} + \frac{\partial u}{\partial y}\frac{\partial v}{\partial y} \\ +\frac{\partial u}{\partial x}\frac{\partial v}{\partial x} + v\frac{\partial^2 v}{\partial x \partial y} \end{bmatrix} \\ +\alpha_2 \begin{pmatrix} 2\frac{\partial u}{\partial x}\frac{\partial u}{\partial y} + \frac{\partial u}{\partial x}\frac{\partial v}{\partial x} \\ +2\frac{\partial v}{\partial y}\frac{\partial u}{\partial y} + 2\frac{\partial v}{\partial x}\frac{\partial v}{\partial y} \end{pmatrix} \end{matrix} & 0 \\ \begin{matrix} \mu\left(\frac{\partial u}{\partial y} + \frac{\partial v}{\partial x}\right) \\ +\alpha_1 \begin{bmatrix} \frac{\partial^2 u}{\partial t \partial y} + \frac{\partial^2 v}{\partial t \partial x} \\ +u\frac{\partial^2 u}{\partial x \partial y} + u\frac{\partial^2 v}{\partial x^2} \\ +v\frac{\partial^2 u}{\partial y^2} + 3\frac{\partial v}{\partial x}\frac{\partial v}{\partial y} \\ +3\frac{\partial u}{\partial x}\frac{\partial u}{\partial y} + \frac{\partial u}{\partial y}\frac{\partial v}{\partial y} \\ +\frac{\partial u}{\partial x}\frac{\partial v}{\partial x} + v\frac{\partial^2 v}{\partial x \partial y} \end{bmatrix} \\ +\alpha_2 \begin{pmatrix} 2\frac{\partial u}{\partial x}\frac{\partial u}{\partial y} + 2\frac{\partial u}{\partial x}\frac{\partial v}{\partial x} \\ +2\frac{\partial u}{\partial y}\frac{\partial v}{\partial y} + 2\frac{\partial v}{\partial x}\frac{\partial v}{\partial y} \end{pmatrix} \end{matrix} & \begin{matrix} 2\mu\frac{\partial v}{\partial y} + \alpha_1 \begin{bmatrix} 2\frac{\partial^2 v}{\partial t \partial y} + 2v\frac{\partial^2 v}{\partial y^2} \\ +2u\frac{\partial^2 v}{\partial x \partial y} + 4\left(\frac{\partial v}{\partial y}\right)^2 \\ +2(\frac{\partial u}{\partial y})^2 + 2\frac{\partial u}{\partial y}\frac{\partial v}{\partial x} \end{bmatrix} \\ +\alpha_2 \left(4\left(\frac{\partial v}{\partial y}\right)^2 + \left(\frac{\partial u}{\partial y} + \frac{\partial v}{\partial x}\right)^2\right) \end{matrix} & 0 \\ 0 & 0 & 0 \end{bmatrix}$$

$$\rho\left(\frac{dv}{dt}\right)_x = \frac{\partial T_{xx}}{\partial x} + \frac{\partial T_{xy}}{\partial y} \tag{1.34}$$

$$\rho\left(\frac{dv}{dt}\right)_y = \frac{\partial T_{yx}}{\partial x} + \frac{\partial T_{yy}}{\partial y} \tag{1.35}$$

By solving above Eqs. (1.34) and (1.35). we get

$$\frac{\partial u}{\partial t}+u\frac{\partial u}{\partial x}+v\frac{\partial u}{\partial y} = =-\frac{1}{\rho}\frac{\partial p}{\partial x}+\nu\left(\frac{\partial^2 u}{\partial x^2}+\frac{\partial^2 u}{\partial y^2}\right)+\frac{\alpha_1}{\rho}\left[\begin{array}{c}\frac{\partial u}{\partial x}\left(13\frac{\partial^2 u}{\partial x^2}+\frac{\partial^2 u}{\partial^2 y}\right)+u\left(\frac{\partial^3 u}{\partial x^3}+\frac{\partial^2 u}{\partial t\partial y^2}\right)\\ +2\frac{\partial^3 u}{\partial t\partial x^2}+v\left(\frac{\partial^3 v}{\partial y^3}+\frac{\partial^3 u}{\partial x^2\partial y}\right)\\ +2\frac{\partial v}{\partial x}\left(2\frac{\partial u^2}{\partial x^2}+\frac{\partial^2 u}{\partial x\partial y}\right)+3\frac{\partial u}{\partial y}\left(\frac{\partial^2 u}{\partial x\partial y}+\frac{\partial v^2}{\partial x^2}\right)\\ +2\frac{\partial^3 u}{\partial t\partial x^2}+\frac{\partial^3 u}{\partial t\partial y^2}+\frac{\partial^3 v}{\partial t\partial x\partial y}\end{array}\right]$$
$$+\frac{2\alpha_2}{\rho}\left[4\frac{\partial u}{\partial x}\frac{\partial^2 u}{\partial x^2}+\frac{\partial u}{\partial y}\left(\frac{\partial^2 u}{\partial x\partial y}+\frac{\partial v^2}{\partial x^2}\right)+\frac{\partial v}{\partial x}\left(\frac{\partial^2 u}{\partial x\partial y}+\frac{\partial v^2}{\partial x^2}\right)\right]-\frac{\sigma B_0^2 u}{\rho}, \quad (1.36)$$

$$\frac{\partial v}{\partial t}+u\frac{\partial v}{\partial x}+v\frac{\partial v}{\partial y} = -\frac{1}{\rho}\frac{\partial p}{\partial y}+\nu\left(\frac{\partial^2 v}{\partial x^2}+\frac{\partial^2 v}{\partial y^2}\right)+\frac{\alpha_1}{\rho}\left[\begin{array}{c}\frac{\partial^3 u}{\partial t\partial x\partial y}+\frac{\partial^3 v}{\partial t\partial y\partial x^2}+2\frac{\partial^3 v}{\partial t\partial y^2}\\ +\frac{\partial v}{\partial y}\left(13\frac{\partial^2 v}{\partial y^2}+\frac{\partial^2 v}{\partial x^2}\right)+u\left(\frac{\partial^3 v}{\partial x^3}+\frac{\partial^2 v}{\partial x\partial y^2}\right)\\ +v\left(\frac{\partial^3 v}{\partial y^3}+\frac{\partial^3 v}{\partial x^2\partial y}\right)+2\left(\frac{\partial u}{\partial y}\frac{\partial^2 u}{\partial y^2}+\frac{\partial^2 v}{\partial x\partial y}\right)\\ +3\left(\frac{\partial v}{\partial x}\frac{\partial^2 v}{\partial x\partial y}+\frac{\partial v^2}{\partial y^2}\right)\end{array}\right]$$
$$+\frac{2\alpha_2}{\rho}\left[4\frac{\partial v}{\partial y}\frac{\partial^2 v}{\partial y^2}+\frac{\partial u}{\partial y}\left(\frac{\partial^2 v}{\partial x\partial y}+\frac{\partial^2 u}{\partial y^2}\right)+\frac{\partial v}{\partial x}\left(\frac{\partial^2 v}{\partial x\partial y}+\frac{\partial^2 u}{\partial x^2}\right)\right]-\frac{\sigma B_0^2 v}{\rho}, \quad (1.37)$$

Using [15]

$$u=O(1), \quad v=O(\delta), \quad x=O(1), \quad y=O(\delta), \quad \frac{T_{xx}}{\rho}=O(1), \quad \frac{T_{xy}}{\rho}=O(\delta), \quad \frac{T_{yy}}{\rho}=O(\delta^2), \quad (1.38)$$

We get

$$\frac{\partial u}{\partial t}+u\frac{\partial u}{\partial x}+v\frac{\partial u}{\partial y}=\nu\frac{\partial^2 u}{\partial x^2}+\frac{k_0}{\rho}\left[\frac{\partial^3 u}{\partial t\partial y^2}+\frac{\partial}{\partial x}\left(u\frac{\partial^2 u}{\partial y^2}\right)+\frac{\partial u}{\partial y}\frac{\partial^2 v}{\partial y^2}+v\frac{\partial^3 u}{\partial y^3}\right]-\frac{\sigma B_0^2}{\rho}u, \quad (1.39)$$

where [16]

$$\mu\geq 0, \quad \alpha_1\geq 0, \quad \alpha_1+\alpha_2=0. \quad (1.40)$$

and now Eq. (1.39) can be written as

$$\frac{\partial u}{\partial t}+u\frac{\partial u}{\partial x}+v\frac{\partial u}{\partial y}=\nu\frac{\partial^2 u}{\partial x^2}+\frac{\alpha_1}{\rho}\left[\frac{\partial u}{\partial x}\frac{\partial^2 u}{\partial y^2}+u\frac{\partial^3 u}{\partial x\partial y^2}+\frac{\partial u}{\partial y}\frac{\partial^2 v}{\partial y^2}+v\frac{\partial^3 u}{\partial y^3}\right]-\frac{\sigma B_0^2}{\rho}u. \quad (1.41)$$

1.17 Finite difference method

Finite difference method is an approximate method in the sense that derivatives at a point are approximated by difference quotient over a small interval. It was first utilized by Euler, probably in 1768.

Assume that function F and its derivatives are single valued, finite and contain fumction of z, then by Tayler's theorem

$$F(z+h) = F(z) + hF'(z) + \frac{h^2}{2}F'(z) + \frac{h^2}{2}F'(z) + 0\left(h^4\right) \tag{1.42}$$

and

$$F(z-h) = F(z) - hF'(z) + \frac{h^2}{2}F'(z) - \frac{h^2}{2}F'(z) + 0\left(h^4\right) \tag{1.43}$$

where $O(h^4)$ denotes term containing fourth and higher power of h. These approximations gives

$$\left(\frac{dF}{dz}\right)_{z=z} \approx \frac{F(z+h) - F(z)}{h} \tag{1.44}$$

$$\left(\frac{dF}{dz}\right)_{z=z} \approx \frac{F(z) - F(z-h)}{h} \tag{1.45}$$

with the error of order h. We assume that containing second and higher power of h are negligible. Eq. (1.44) and Eq. (1.45) are called forward and backward difference formulae. Subtracted Eq. (1.43)from Eq. (1.42) gives

$$\left(\frac{dF}{dz}\right)_{z=-z} \approx \frac{F(z+h) - F(z-h)}{2h} \tag{1.46}$$

with leading error of h^2. This approximation is called central difference formula. Similarly we can find the approximation for second and third derivatives.

Chapter 2

Hydromagnetic flow in a viscoelastic fluid over an oscillatory stretching surface

2.1 Introduction

This chapter deals with the unsteady MHD two-dimensional boundary layer flow of a second grade fluid due to an oscillatory stretching surface. An infinite elastic sheet is stretched back and forth in its own plane. The resulting flow equations are transformed to a non-linear partial differential equations by invoking similarity transformations. Numerical solution is developed by using the finite difference scheme, in which a coordinate transformation is employed to transform the semi-infinite physical space to a bounded computational domain. The influence of the various parameters like viscoelastic parameter, the hartmann number, the relative frequency amplitude of the oscillatory stretching sheet to the stretching rate on the velocity field and the wall shear stress are plotted and analyzed through graphs and tables. This paper is a review of the work done by Abbas et al. [14].

2.2 Flow Analysis

We consider the unsteady two dimensional magnetohydrodynamics (MHD) laminar flow of incompressible viscoelastic fluid (second grade fluid) over an oscillatory stretching sheet coinciding with plane $\overline{y} = 0$, the flow is being confined to the semi-infinte space $\overline{y} > 0$. The elastic sheet is stretched back and forth periodically with velocity $u_w = b\overline{x}sin\omega t$ (b is maximum stretching rate, $\overline{x}$ is coordinate along sheet and ω is frequency) parallel to the $\overline{x}$ axis, as shown in Fig. 2.1. A constant magnetic field of strength B_0 is applied perpendicular to the stretching surface and the induced magnetic field is neglected, which is valid assumption on a laboratory scale under the assumption of small magnetic Reynolds number. Under the usual boundary layer assumptions and in the absence of pressure gradient, the unsteady basic boundary layer equations governing the MHD flow of second grade fluid are:

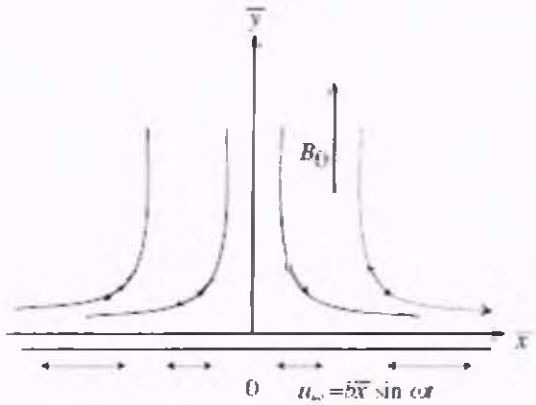

Fig. 2.1: Geometry of the problem

$$\frac{\partial u}{\partial \overline{x}} + \frac{\partial v}{\partial \overline{y}} = 0, \tag{2.1}$$

$$\frac{\partial u}{\partial t} + u\frac{\partial u}{\partial \overline{x}} + v\frac{\partial u}{\partial \overline{y}} = \nu\frac{\partial^2 u}{\partial \overline{y}^2} + \frac{k_0}{\rho}\left[\frac{\partial^3 u}{\partial t \partial \overline{y}^2} + \frac{\partial}{\partial \overline{x}}\left(u\frac{\partial^2 u}{\partial \overline{y}^2}\right) + \frac{\partial u}{\partial \overline{y}}\frac{\partial^2 v}{\partial \overline{y}^2} + v\frac{\partial^3 u}{\partial \overline{y}^3}\right] - \frac{\sigma B_0^2}{\rho}u. \tag{2.2}$$

where (u, v) are the velocity component in $(\overline{x}, \overline{y})$ directions, respectively, ν is the kinematic viscosity of fluid, ρ is the fluid density, σ is the electrical conductivity of fluid and k_0 is the viscoelastic parameter of fluid.

The appropriate boundary conditions of the problem are

$$u = u_\omega = b\overline{x}\sin\omega t, \quad v = 0 \quad \text{at} \quad \overline{y} = 0, \quad t > 0. \tag{2.3}$$

$$u = 0, \quad \frac{\partial u}{\partial \overline{y}} = 0 \quad \text{as} \quad \overline{y} \to \infty, \tag{2.4}$$

in which b and ω have the dimensions $(\text{time})^{-1}$. Note that the system can also be solved by using the cosine function $(\cos\omega t)$ instead of $\sin\omega t$. The second condition in Eq. (2.4) is augmented condition since the flow is in an unbounded domain, which has been discussed by Garg and Rajagopal [5] . Now we assume

$$S \equiv \frac{\omega}{b}, \tag{2.5}$$

which is the ratio of the oscillation frequency of the sheet to its stretching rate.

Any particle path on the sheet is

$$\overline{x} = \overline{x}_o \exp\left(\frac{1}{S}\cos\omega t\right). \tag{2.6}$$

To simplify the flow equations, we use the following similarity transformations

$$\begin{aligned} y &= \sqrt{\frac{b}{\nu}}\overline{y}, \quad \tau = t\omega, \\ u &= b\overline{x} f_y(y, \tau), \quad v = -\sqrt{\nu b} f(y, \tau). \end{aligned} \tag{2.7}$$

Using Eq. (2.7), the continuity equation (2.1) is identically satisfied and the governing Eq. (2.2) becomes

$$S f_{y\tau} + f_y^2 - f f_{yy} + M^2 f_y = f_{yyy} + K\left(S f_{yyy\tau} + 2 f_y f_{yyy} - f_{yy}^2 - f f_{yyyy}\right), \tag{2.8}$$

subject to the boundary conditions

$$\begin{aligned} f_y(0,\tau) &= \sin\tau, \qquad f(0,\tau)=0, \\ f_y(\infty,\tau) &= 0 \ \text{ and } \ f_{yy}(\infty,\tau)=0, \end{aligned} \tag{2.9}$$

in which $M^2 = \sigma B_0^2/b\rho$ is the Hartmann number or magnetic parameter and $K = bk_0/\nu b$ is non-dimensional viscoelastic parameter. Here $K = 0$ corresponds to the case of Newtonian fluid.

A physical quantity of interest is the skin-friction coefficient C_f, which is defined as

$$C_f = \frac{\tau_w}{\rho u_w^2}, \tag{2.10}$$

where τ_w is wall shear stress and is given by

$$\tau_w = \mu\left(\frac{\partial u}{\partial \overline{y}}\right)_{\overline{y}=0} + k_0\left(\frac{\partial^2 u}{\partial t\partial \overline{y}} + u\frac{\partial^2 u}{\partial \overline{x}\partial \overline{y}} + v\frac{\partial^2 u}{\partial \overline{y}^2} - 2\frac{\partial u}{\partial \overline{y}}\frac{\partial v}{\partial \overline{y}}\right)_{\overline{y}=0}. \tag{2.11}$$

Using Eq. (2.7) and (2.11), Eq. (2.10) yields

$$Re_x^{1/2} C_f = \left[f_{yy} + K\left(3f_y f_{yy} + S f_{yy\tau} - f f_{yyy}\right)\right]_{y=0}, \tag{2.12}$$

where $Re_x = u_w \overline{x}/\nu$ is the local Reynolds number.

2.3 Solution of the Problem

The non linear boundary-value problem consisting of Eq. (2.8) with the boundary conditions Eq. (2.9) is solved by means of the finite difference method. For this purpose, the coordinate transformation $\eta = 1/(y+1)$ is applied for transforming the semi-infinite physical domain $y \in [0,\infty)$ to a finite calculation domain $\eta \in [0,1]$, i.e.

$$y = \frac{1}{\eta} - 1, \qquad \frac{\partial}{\partial y} = -\eta^2\frac{\partial}{\partial \eta}, \qquad \frac{\partial^2}{\partial y^2} = \eta^4\frac{\partial^2}{\partial \eta^2} + 2\eta^3\frac{\partial}{\partial \eta}, \qquad \frac{\partial^2}{\partial y\partial \tau} = -\eta^2\frac{\partial^2}{\partial \eta\partial \tau},$$

$$\frac{\partial^3}{\partial y^3} = -\eta^6\frac{\partial^3}{\partial \eta^3} - 6\eta^5\frac{\partial^2}{\partial \eta^2} - 6\eta^4\frac{\partial}{\partial \eta}, \qquad \frac{\partial^4}{\partial y^3\partial \tau} = -\eta^6\frac{\partial^4}{\partial \eta^3\partial \tau} - 6\eta^5\frac{\partial^3}{\partial \eta^2\partial \tau} - 6\eta^4\frac{\partial^2}{\partial \eta\partial \tau},$$

$$\frac{\partial^4}{\partial y^4} = \eta^8 \frac{\partial^4}{\partial \eta^4} + 12\eta^7 \frac{\partial^3}{\partial \eta^3} + 35\eta^6 \frac{\partial^2}{\partial \eta^2} + 24\eta^5 \frac{\partial}{\partial \eta}. \tag{2.13}$$

Using the above transformations, the Eq. (2.8) can be written in the form of η as

$$\begin{aligned} & S\left(1-6K\eta^2\right)\frac{\partial^2 f}{\partial \tau \partial \eta} - SK\eta^4 \frac{\partial^4 f}{\partial \eta^3 \partial \tau} - 6SK\eta^3 \frac{\partial^3 f}{\partial \eta^2 \partial \tau} \\ = \; & \left(\eta^2 - 8K\eta^4\right)\left(\frac{\partial f}{\partial \eta}\right)^2 + \left(6\eta^2 - M^2 + 36Kf\eta^4 - 2f\eta\right)\frac{\partial f}{\partial \eta} + \eta^4 \frac{\partial^3 f}{\partial \eta^3} \\ & + \left(6\eta^3 - f\eta^2 + 36Kf\eta^4\right)\frac{\partial^2 f}{\partial \eta^2} - 8K\eta^5 \frac{\partial f}{\partial \eta}\frac{\partial^2 f}{\partial \eta^2} + K\eta^6\left(\frac{\partial^2 f}{\partial \eta^2}\right)^2 \\ & -2K\eta^6 \frac{\partial f}{\partial \eta}\frac{\partial^3 f}{\partial \eta^3} + 12K\eta^5 f\frac{\partial^3 f}{\partial \eta^3} + K\eta^6 f\frac{\partial^4 f}{\partial \eta^4}. \end{aligned} \tag{2.14}$$

The boundary conditions (2.9) in terms of η can be written as

$$f_\eta = 0, \qquad f_{\eta\eta} = 0 \quad \text{at} \quad \eta = 0, \tag{2.15}$$

$$f = 0, \quad f_\eta = -\sin\tau \quad \text{at} \quad \eta = 1. \tag{2.16}$$

The equation (2.14) is a differential equation, we can discretise it for L uniformly distributed discrete points in $\eta = \left(\eta,\ \eta,\ \eta_3,\ \ldots\ldots,\ \eta_{\{L\}}\right) \in (0,1)$ with a space grid size of $\Delta\eta = 1/(L+1)$ and the time levels $t = \left(t^1,\ t^2, \ldots\right)$. Hence the discrete values $(f_1^n,\ f_2^n,\ \ldots\ldots,\ f_L^n)$ at these grid points for the time step $t^n = n\Delta t$ (where Δt is time step size) can be numerically solved together with the boundary conditions at $\eta = \eta_0 = 0$ and $\eta = \eta_{\{L+1\}} = 1$, Eqs. (2.15) and (2.16) as the initial conditions are given as

$$f\left(\eta, \tau = 0\right) = 0. \tag{2.17}$$

We will see that periodic function will be immediately reached within the first period. we construct a semi-implicite time difference for f and assure that only linear equation for the

new time step $(n+1)$ need to be solved.

$$
\begin{aligned}
& S(1-6K\eta^2)\frac{1}{\Delta t}\left(\frac{\partial f^{(n+1)}}{\partial \eta}-\frac{\partial f^{(n)}}{\partial \eta}\right)-SK\eta^4\frac{1}{\Delta t}\left(\frac{\partial^3 f^{(n+1)}}{\partial \eta^3}-\frac{\partial^3 f^{(n)}}{\partial \eta^3}\right) \\
& -6SK\eta^3\frac{1}{\Delta t}\left(\frac{\partial^2 f^{(n+1)}}{\partial \eta^2}-\frac{\partial^2 f^{(n)}}{\partial \eta^2}\right) \\
= \; & \left(\eta^2-8K\eta^4\right)\left(\frac{\partial f^{(n)}}{\partial \eta}\right)^2+\left(6\eta^2-M^2\right)\frac{\partial f^{(n+1)}}{\partial \eta}+\left(36K\eta^4-2\eta\right)f^{(n)}\frac{\partial f^{(n)}}{\partial \eta}+6\eta^3\frac{\partial^2 f^{(n+1)}}{\partial \eta^2} \\
& +\left(36K\eta^4-\eta^2\right)f^{(n)}\frac{\partial^2 f^{(n)}}{\partial \eta^2}-8K\eta^5\frac{\partial f^{(n)}}{\partial \eta}\frac{\partial^2 f^{(n)}}{\partial \eta^2}+K\eta^6\left(\frac{\partial^2 f^{(n)}}{\partial \eta^2}\right)^2+\eta^4\frac{\partial^3 f^{(n+1)}}{\partial \eta^3} \\
& -2K\eta^6\frac{\partial f^{(n)}}{\partial \eta}\frac{\partial^3 f^{(n)}}{\partial \eta^3}+12K\eta^5 f^{(n)}\frac{\partial^3 f^{(n)}}{\partial \eta^3}+K\eta^6 f^{(n)}\frac{\partial^4 f^{(n)}}{\partial \eta^4}. \qquad (2.18)
\end{aligned}
$$

It should be noted that other time differences are also mean of finite difference method we can obtained a linear equation system for each step, which can be solved e.g. by Gaussian elimination.

2.4 Results and Discussion

We calculate the velocity field by solving Eq. (2.8) with boundary conditions Eq.(2.9) by using finite difference method. First the initial boundary value problem in the computational space $\eta \in [0,1]$ and then the numerical solutions are transformed to the physical space with y-coordinate $y \in [0,\infty)$. The velocity field $f' = (f_y)$ is plotted for the various parameters, for example, the viscoelastic parameter K, the Hartmann number or magnetic parameter M and the non-dimensional relative amplitude of frequency to the stretching rate S, for the time series of the first five periods $\tau \in [0, 10\pi]$ and the transverse profiles. We also calculate and show the values of the skin-friction coefficient $Re_x^{1/2}C_f$ both graphically and in tabular form.

Fig. 2.2 is plotted to examine the effects of the time series of velocity field f' at four different distances from the oscillating sheet far the first five periods $\tau \in [0, 10\pi]$ by keeping $K = 0.1$ and $K = 0.4$. In Fig. 2.2(a) (at $K = 0.1$) that the amplitude of flow near the oscillating surface is larger as compared to that for away from surface. However, in Fig. 2.2(b) (for $K = 0.4$) the amplitude of flow motion is larger as compared with analysis at $K = 0.1$. That shows as

increased effective viscosity with the increase of the non-Newtonian parameter K.

Fig. 2.3 illustrates the effects of non-dimentional relative amplitude of frequency to the stretching rate S, the viscoelastic parameter K and magnetic parameter M on the time series of the velocity field $f^{'}$ at the fixed distance $y = 0.25$ from the surface, respectively. Fig. 2.3 (a) shows that with the increase of S the amplitude of fiow increases slightly and a phase shift occurs which increases with the increase of S. The variation of the viscoelastic parameter K on the time series of velocity $f^{'}$ can be seen from Fig. 2.3(b) with fixed values of $S = 2$ and $M = 10$. We note that amplitude of the flow motion is increased by increasing the viscoelastic parameter K due to the increased effective viscosity. Fig. 2.3(c) shows the time series of velocity profile $f^{'}$ for different values of the magnetic parameter M with fixed values of $S = 1$ and $K = 0.2$. As expected, the amplitude of flow decreases with the increase of magnetic parameter M. This is because for the investigated problem the magnetic force act as resistance to the flow.

Fig. 2.4 gives the effects of viscoelastic parameter K on the transverse profile of velocity $f^{'}$ for the different times of $\tau = 8.5\pi$, 9π, 9.5π and 10π in the fifth period $\tau \in [8\pi, 10\pi]$ for which a periodic motion has been reached. Fig. 2.4(a) (a) shows that at $\tau = 8.5\pi$, $f^{'} = 1$ at the surface $y = 0$ equating the sheet velocity and $f^{'} \to 0$ far away from the sheet. It can also be seen that at this point of time, there is no oscillation in velocity profile and $f^{'}$ is increased as value of K increases, i.e. the boundary layer become thickener with increase of K. Fig. 2.8(b) gives the velocity profile $f^{'}$ at time point $\tau = 9\pi$. At this point the velocity field $f^{'}$ is zero at the surface $y = 0$ and far away from the wall it again approaches to zero. It is also evident that near the wall, there exist some oscillation in the velocity profile and the amplitude of flow increases as K increases. This oscillation in transverse profile is an evdient of phase shift in the viscoelastic fluid against the viscous Newtonian fluid ($K = 0$). The velocity profile for other two time points within fifth period are displayed in Fig. 2.4$(c) - (d)$.

Fig. 2.5 gives the influence of the magnetic parameter M on the transverse profile of the velocity field $f^{'}$ for the different times of $\tau = 8.5\pi$, 9π, 9.5π and 10π. It is noted that the influence of magnetic field reduces the boundary layer thickness. As expected magnetic force is a resistance to the flow, hence reduces the velocity magnitude. Although for $\tau = 9\pi$ (Fig. 2.5(b)) and $\tau = 10\pi$ (Fig. 2.5(d)), there exist still velocity oscillation in the transverse profile , their amplitudes are fairly small (in comparison with those in Fig. 2.3 (b, d)

Fig. 2.6 elucidates the effect of non-dimentional relative amplitude of frequency to the stretching rate S on the velocity f' for the different times of $\tau = 8.5\pi$, 9π, 9.5π and 10π in the fifth period. Fig. 2.6(a) is plotted for the variation of S on the velocity f' at time $\tau = 8.5\pi$ at the surface. It is observed that the velocity is equal to the sheet velocity $f' = 1$ at surface $y = 0$ and far away from the wall it is zero. The velocity f' increases only slightly with the increase of S. Fig. 2.6(b) shows the influence of S on the velocity field f' at time $\tau = 9\pi$. It is noted that for very small values of $S = 0.1$ at this time point, the velocity in the transverse section takes its value at the plate almost to the zero ($f' \to 0$), i.e., for small value of S no phase difference occurs with increase of the distance from the plate and the flow in the whole flow domain is in phase with the sheet motion. The velocity profiles for others two time points within fifth period are plotted in Figs. 2.6(c) and (d) and the similar observations are noted as in Fig. 2.6(a) and (b), respectively.

Fig. 2.7 depicts the variation of viscoelastic parameter K, the relative amplitude of frequency to the stretching rate S and the magnetic parameter M on the skin friction coefficient $Re_x^{1/2}C_f$ for the time series in the first five periods $\tau \in [0, 10\pi]$. Fig. 2.7(a) shows the influence of the viscoelastic parameter K on the skin friction coefficient $Re_x^{1/2}C_f$ with fixed $S = 5$ and $M = 12$. It is found that the skin friction coefficient varies also periodically due to oscillatory surface motion. The oscillation amplitude of skin friction coefficient $Re_x^{1/2}C_f$ increases as the values of K are increased. Fig. 2.7(b) shows the variation of S on the skin-friction coefficient $Re_x^{1/2}C_f$. It can be seen that the oscillation amplitude of skin friction coefficient increases by increasing the values of S. Fig. 2.7(c) displays the results of the magnetic number M on the skin friction coefficient $Re_x^{1/2}C_f$ with fixed $S = 1$ and $K = 0.1$. It is noted that the oscillation amplitude of the skin friction coefficient $Re_x^{1/2}C_f$ is increased with an increase in M.

Table 2.1 gives the numerical values of skin friction coefficient $Re_x^{1/2}C_f$ on the different values of K, S and M at the different periods of time series. The results show that the values of the skin friction coefficient for the three different time points $\tau = 1.5\pi$, 5.5π and 9.5π are almost identical. It means that the periodic motion may be reached within first period when the initial conditions are set up. The change of the skin friction coefficient from positive to negative with increase of K as shown in Fig. 2.7(a)(but for slightly different parameters). It is also found that the values of the skin friction coefficient are increased as the relative frequency

to the stretching rate S or/and magnetic field M are increased.

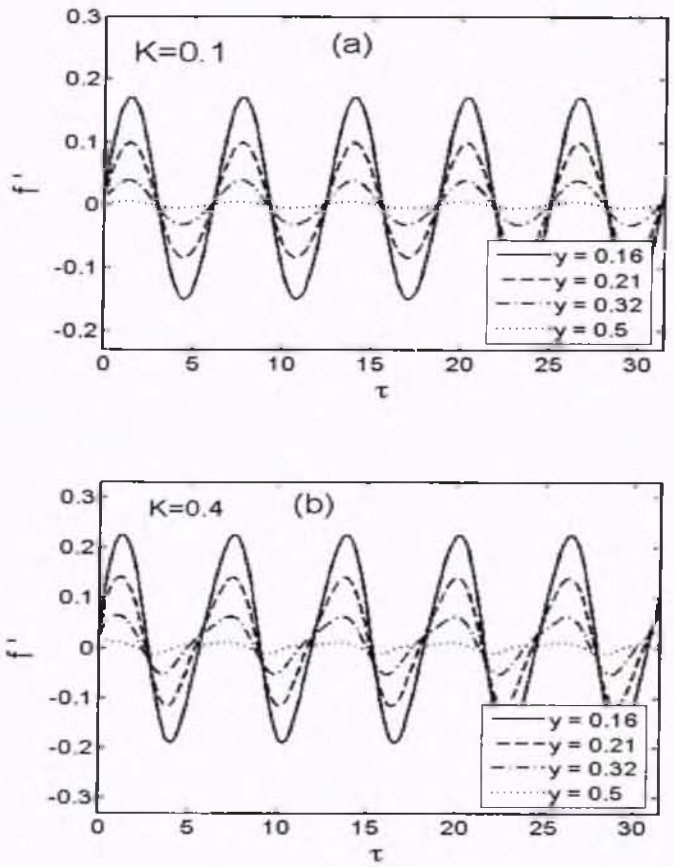

Fig. 2.2: Time series of the flow of the velocity field f' at the four different distances from the surface for the time period $\tau \in [0, 10\pi]$ with $S = 2$, $M = 10$: (a) $K = 0.1$ and (b) $K = 0.4$.

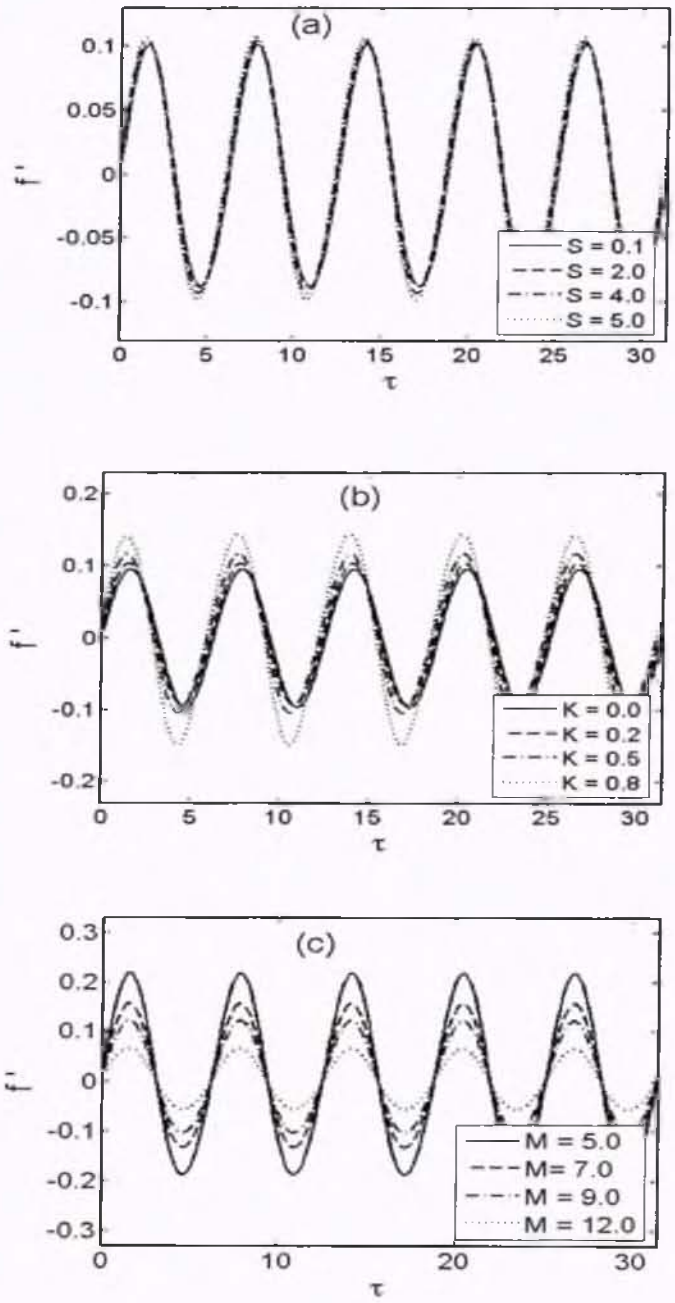

Fig. 2.3: Time series of the velocity field f' in first five periods $\tau \in [0, 10\pi]$ at a fixed distance to the sheet, $y = 0.25$: (a) effects of S with $K = 0.2$, $M = 10$. (b) effects of viscoelastic parameter K with $S = 2$, $M = 10$ and (c) effects of magnetic parameter M with $S = 1$, $K = 0.2$.

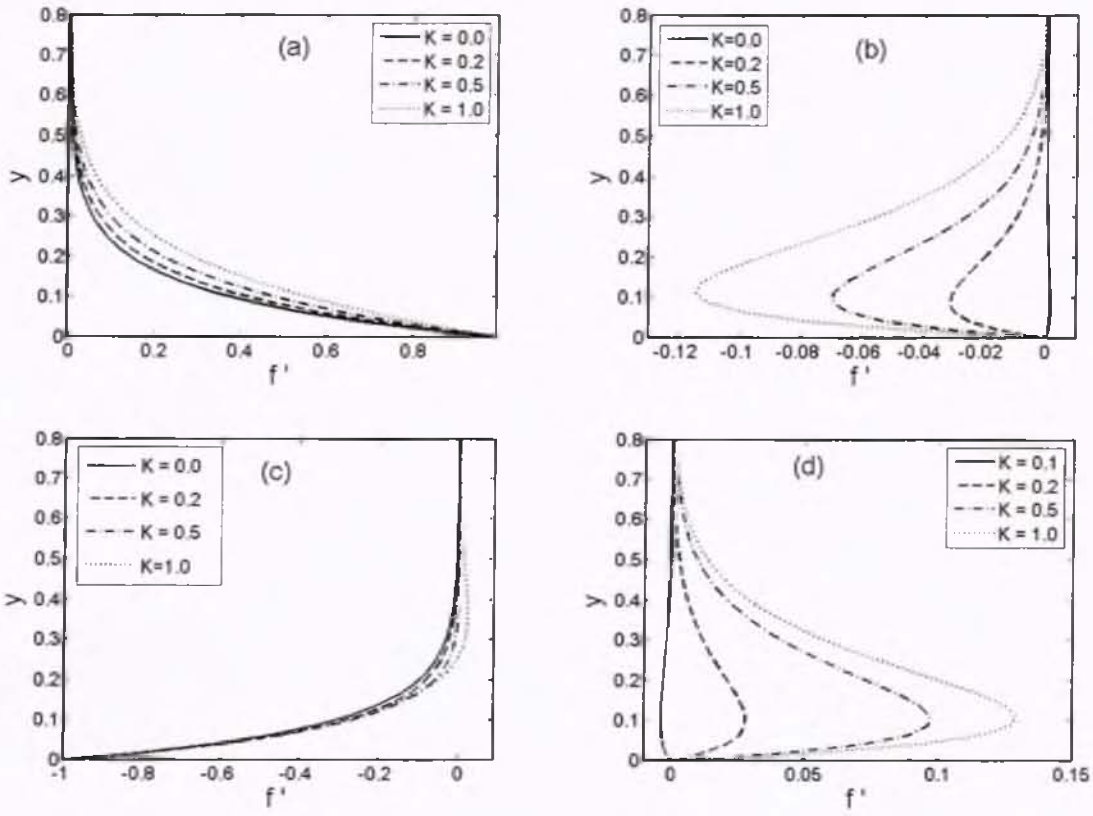

Fig. 2.4: Transverse profiles of the velocity field f' at the four different values of K for the fifth period $\tau \in [8\pi, 10\pi]$ for which a periodic velocity field has been reached: (a) $\tau = 8.5\pi$, (b) $\tau = 9\pi$ (c) $\tau = 9.5\pi$ and (d) $\tau = 10\pi$ with $S = 2$, $M = 10$.

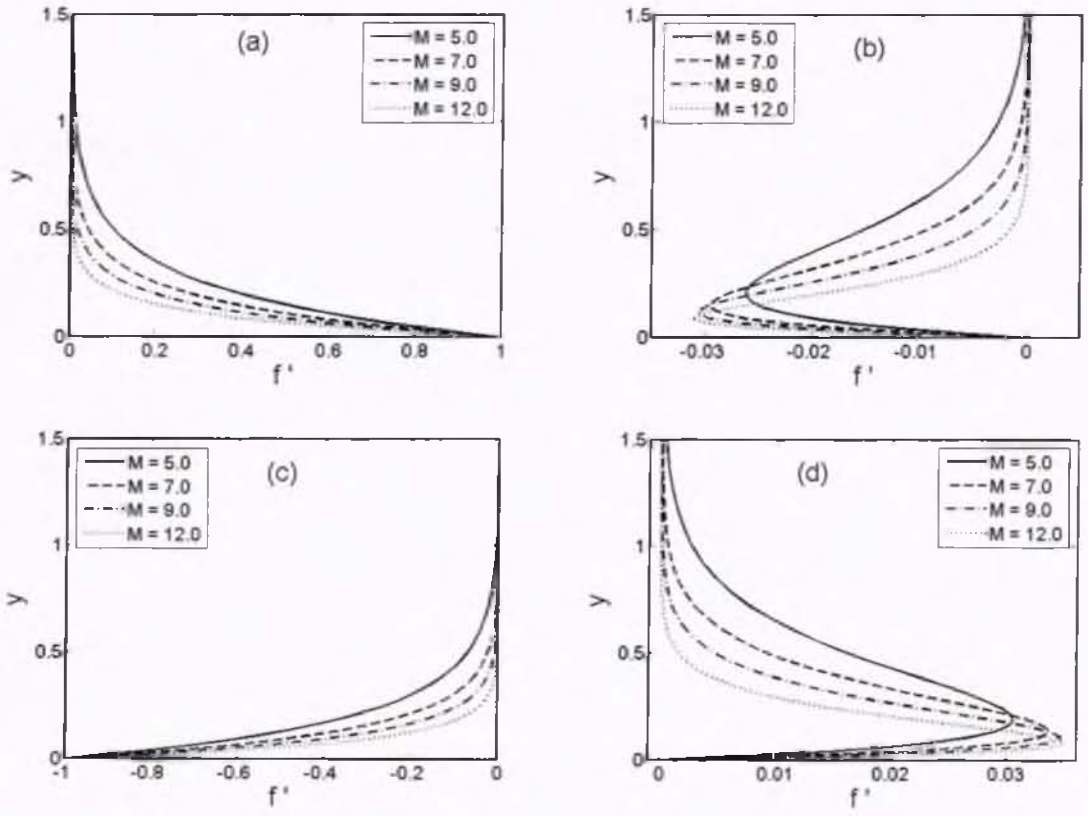

Fig. 2.5: Transverse profiles of the velocity field f' at the four different values of M for the fifth period $\tau \in [8\pi, 10\pi]$ for which periodic velocity field has been reached: (a) $\tau = 8.5\pi$, (b) $\tau = 9\pi$, (c) $\tau = 9.5\pi$ and (d) $\tau = 10\pi$ with $S = 1$, $K = 0.2$.

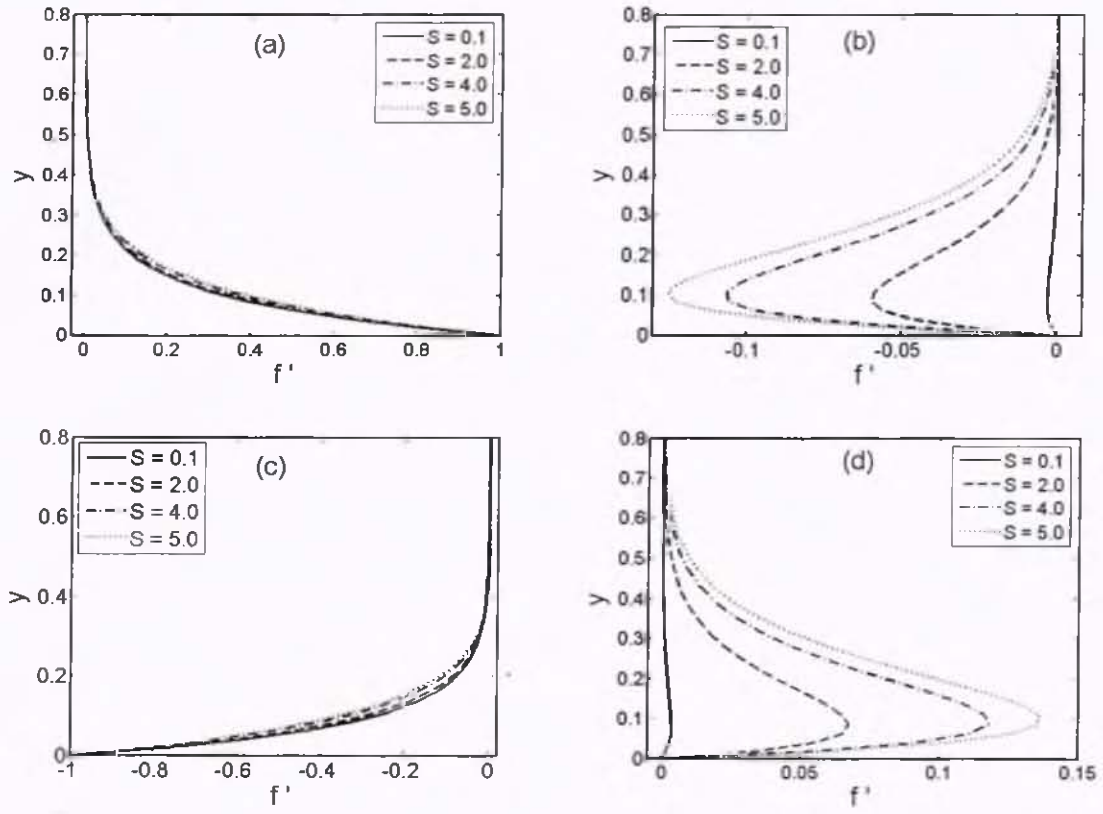

Fig. 2.6: Transverse profiles of the velocity field f' at the four different values of S for the fifth period $\tau \in [8\pi, 10\pi]$ for which a periodic velocity field has been reached: (a) $\tau = 8.5\pi$, (b) $\tau = 9\pi$, (c) $\tau = 9.5\pi$ and (d) $\tau = 10\pi$ with $K = 0.2$, $M = 12$.

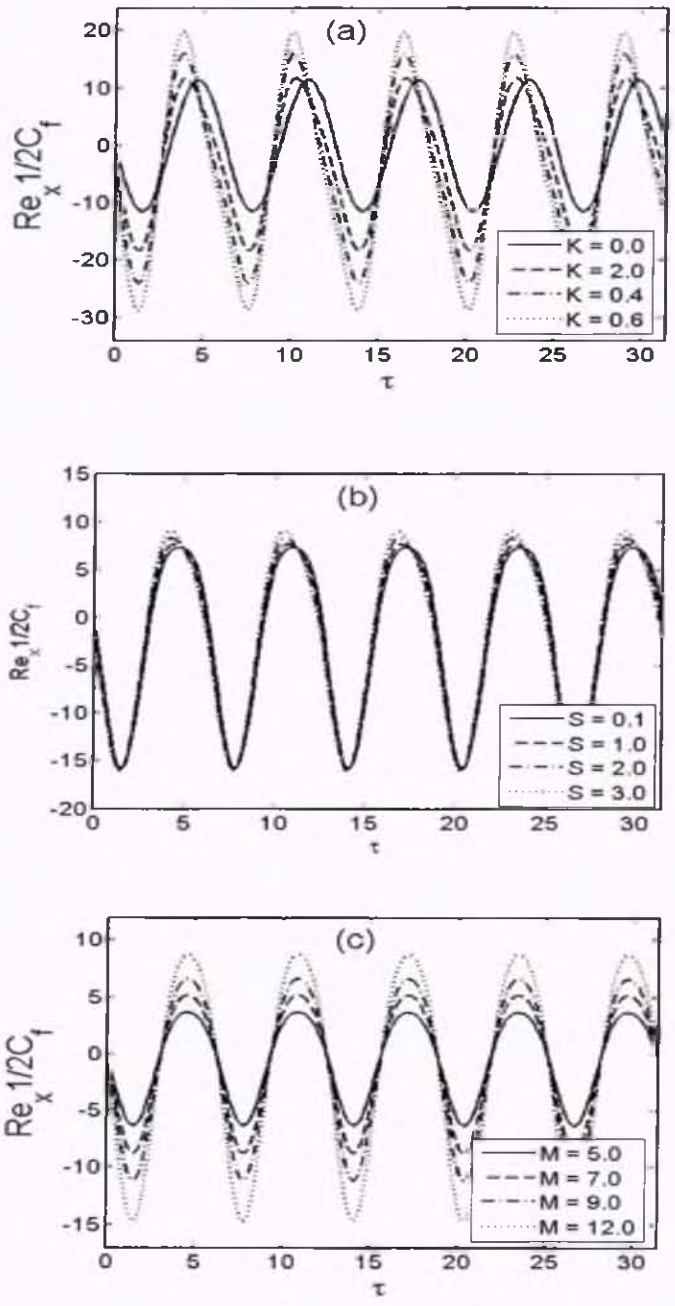

Fig. 2.7: Time series of the skin friction coefficient $Re_x^{1/2}C_f$ in the first five periods $\tau \in [0, 10\pi]$: (a) effects of K with $S = 5$, $M = 12$, (b) effects of S with $K = 0.1$, $M = 12$ and (c) effects of M with $K = 0.1$, $S = 1$.

Table 2.1: Numerical values of the skin-friction coefficient $Re_x^{1/2}C_f$ for different values of K, S, and M at three different time points $\tau = 1.5\pi$, $\tau = 5.5\pi$ and $\tau = 9.5\pi$.

K	S	M	$\tau = 1.5\pi$	$\tau = 5.5\pi$	$\tau = 9.5\pi$
0.0	1.0	12.0	11.678656	11.678707	11.678656
0.2			5.523296	5.523371	5.523257
0.5			-3.899067	-3.899262	-3.899162
0.8			-11.674383	-11.676506	-11.676116
1.0			-15.617454	-15.624607	-15.624963
0.2	0.5		5.322161	5.322193	5.322173
	1.0		5.523296	5.523371	5.523257
	2.0		6.08707	6.087031	6.087156
	3.0		6.769261	6.768992	6.769294
	4.0		7.497932	7.496924	7.496870
	5.0		8.232954	8.229085	8.228996
	1.0	5.0	2.323502	2.323551	2.323548
		7.0	3.278018	3.278005	3.278123
		9.0	4.197624	4.197771	4.197733
		12.0	5.523296	5.523371	5.523257
		15.0	6.791323	6.791301	6.791278

Chapter 3

MHD flow and heat transfer over a porous oscillating stretching surface in a viscoelastic fluid

3.1 Introduction

This chapter concerns with the heat transfer of an unsteady two-dimensional and magneto-hydrodynamics (MHD) boundary layer flow of a second grade fluid past a porous oscillating stretching surface. By similarity transformations, the governing flow equations are reduced to a system of non-linear partial differential equations. This system has been solved numerically using the finite difference scheme, in which a coordinate transformation is used to transform the semi-infinite physical space to a bounded computational domain. The influences of the involved parameters on the flow, the temperature distribution, the skin-friction coefficient and the local Nusselt number are shown and discussed in detail. In fact, this chapter is an extension of the work done by Abbas et al. [14].

3.2 Flow analysis

Consider the unsteady two dimensional magnetohydrodynamics (MHD) flow of incompressible viscoelastic fluid (second grade fluid) over a porous oscillatory stretching sheet coinciding with

plane $\overline{y} = 0$. The temperature of the outside surface of the sheet is maintained at a constant temperature of T_w and far away from the sheet the temperature of ambient fluid is T_∞, where $T_w > T_\infty$. Under these assumptions along with the boundary layer approximations, the governing equations far law of conservation of mass, momentum and energy in absence of viscus dissipation are:

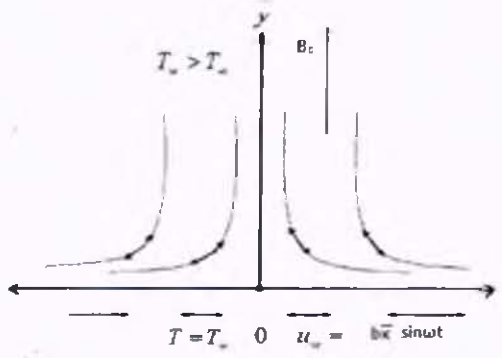

Fig 3.1: Geometry of the problem

$$\frac{\partial u}{\partial \overline{x}} + \frac{\partial v}{\partial \overline{y}} = 0, \tag{3.1}$$

$$\frac{\partial u}{\partial t} + u\frac{\partial u}{\partial \overline{x}} + v\frac{\partial u}{\partial \overline{y}} = \nu\frac{\partial^2 u}{\partial \overline{y}^2} + \frac{k_0}{\rho}\left[\frac{\partial^3 u}{\partial t \partial \overline{y}^2} + \frac{\partial}{\partial \overline{x}}\left(u\frac{\partial^2 u}{\partial \overline{y}^2}\right) + \frac{\partial u}{\partial \overline{y}}\frac{\partial^2 v}{\partial \overline{y}^2} + v\frac{\partial^3 u}{\partial \overline{y}^3}\right] - \frac{\sigma B_0^2}{\rho}u, \tag{3.2}$$

$$\rho c_p\left(\frac{\partial T}{\partial t} + u\frac{\partial T}{\partial \overline{x}} + v\frac{\partial T}{\partial \overline{y}}\right) = k\frac{\partial^2 T}{\partial \overline{y}^2}, \tag{3.3}$$

where c_p is the specific heat at constant pressure, k is the thermal conductivity and T is the temperature of fluid.

The appropriate boundary conditions of the problem are

$$u = u_\omega = b\overline{x}\sin\omega t, \quad v = v_w, \; T = Tw \quad \text{at} \quad \overline{y} = 0, \; t > 0. \tag{3.4}$$

$$u = 0, \quad \frac{\partial u}{\partial \overline{y}} = 0 \quad T \to T_\infty \quad \text{at} \quad y \to \infty, \tag{3.5}$$

where v_w is the wall mass transfer velocity with $(v_w < 0)$ is for suction, and $(v_w > 0)$ is for injunction, respectively. The second condition in (3.5) is arugmented condition since the flow is in unbounded domain and $S \equiv \frac{\omega}{b}$, is defined in previous chapter.

To non-dimentionalize the flow problem, we use the similarity transformations defined in Eq.(2.7) and

$$\theta(y,\tau) = \frac{(T - T_\infty)}{(T_w - T_\infty)}. \tag{3.6}$$

With the help of Eq. (2.7) and Eq. (3.6), the continuity equation is identically satisfied and Eqs. (3.2) and (3.3) give

$$Sf_{y\tau} + f_y^2 - ff_{yy} + M^2 f_y = f_{yyy} + K\left(Sf_{yyy\tau} + 2f_y f_{yyy} - f_{yy}^2 - ff_{yyyy}\right), \tag{3.7}$$

$$\theta_{yy} + Pr\left(f\theta_y - S\theta_\tau\right) = 0, \tag{3.8}$$

subject to the boundary conditions

$$f_y(0,\tau) = \sin\tau, \quad f(0,\tau) = \gamma, \quad \theta(0,\tau) = 1, \tag{3.9}$$

$$f_y(\infty,\tau) = 0, \quad f_{yy}(\infty,\tau) = 0, \quad \theta(\infty,\tau) = 1, \tag{3.10}$$

where $\gamma = -v_w/\sqrt{\nu b}$ is constant with $(\gamma > 0)$ is for suction and $(\gamma < 0)$ is for injection and $\mathrm{Pr} = \mu c_p/k$ is the Prandtl number

The physical quantities of interest are the skin-friction coefficient C_f and the local Nusselt number Nu_x, which are defined as

$$C_f = \frac{\tau_w}{\rho u_w^2}, \qquad Nu_x = \frac{\bar{x} q_w}{k\left(T_w - T_\infty\right)} \tag{3.11}$$

where τ_w and q_w are the shear stress and heat flux at wall, respectively, which are defined as

$$\tau_w = \mu\left(\frac{\partial u}{\partial \bar{y}}\right)_{y=0}, \qquad q_w = -k\left(\frac{\partial T}{\partial \bar{y}}\right)_{\bar{y}=0}. \tag{3.12}$$

Using Eqs. (2.7), (3.6) and Eq. (3.11), Eq. (3.12) gives

$$Re_x^{1/2} C_f = [f_{yy} + K(3 f_y f_{yy} + S f_{yy\tau} - f f_{yyy})]_{\overline{y}=0}, \quad Re_x^{-1/2} Nu_x = -\theta_y(0,\tau) \tag{3.13}$$

where $\mathrm{Re}_x = u_w \overline{x}/\nu$ is the local Reynold number.

3.3 Solution of the problem

We solve the non-linear boundary value problem consisting of Eqs. (3.7) and (3.8) with the boumdary conditions (3.9) and (3.10) using finite difference method. For this purpose, we have been used the same coordinate transformation $\eta = 1/y + 1$ (as used in chapter 2) to transform the semi-infinite physical domain $y \in [0, \infty)$ to finite calculation domain $\eta \in [0, 1]$. Using. Eq. (2.13), the Eq. (3.7) will be same as in the previous chapter and Eq. (3.8) can be written in the form of η as

$$\eta^4 \frac{\partial^2 \theta}{\partial \eta^2} + 2\eta^3 \frac{\partial \theta}{\partial \eta} - Pr(f\eta^2 \frac{\partial \theta}{\partial \eta} + S\frac{\partial \theta}{\partial \tau}) = 0, \tag{3.14}$$

and

$$f_\eta = 0, \quad f_{\eta\eta} = 0, \quad \theta = 0 \quad \text{at} \quad \eta = 0 \tag{3.15}$$

$$f = \gamma, \quad f_\eta = -\sin\tau, \quad \text{at} \quad \theta = 1 \quad \eta = 1 \tag{3.16}$$

Because Eqs. (2.14) and (3.14) are differential equations, we can discretize them for L uniformly distributed discrete points in $\eta = \left(\eta_1, \eta_2, ..., \eta_{\{L\}}\right) \in (0,\ 1)$ with a space grid size of $\Delta\eta = 1/(M+1)$ and time level $t = \left(t^1,\ t^2, ...\right)$. Hence the discrete values $(f_1^n,\ f_2^n,\ .....,\ f_L^n)$ and $(\theta_1^n,\ \theta_2^n,\ .....,\ \theta_L^n)$ at these grid point for time levels $t^n = n\Delta t$ (Δt is the time step size) can be numerically solved together with boundary conditions at $\eta = \eta_0 = 0$ and $\eta = \eta_{\{L+1\}} = 1$, (3.15) and (3.16), as the initial conditions are given. We start our simulations from a motionless velocity field and a uniform temperature distribution equal to temperature at infinity

$$f(\eta, \tau = 0) = 0 \quad \text{and} \quad \theta(\eta, \tau = 0) = 0. \tag{3.17}$$

The oscillatory motion of the sheet with a temperature T_w ($\theta = 1$) is suddenly set from $\tau = 0$ at $\eta = 1$ ($y = 0$). We will see that this periodic motion will be immediately reached within first

period. We construct a semi-infinite time difference for f and θ, respectively, and make sure that only linear equations for the new time step $(n+1)$ need to be solved. The equation of the velocity field for new time step $(n+1)$ will similar to Eq. (2.18) and Eq.(3.14) becomes

$$SPr\frac{\left(\theta^{(n+1)}-\theta^{(n)}\right)}{\Delta t}=\eta^4\frac{\partial^2\theta^{(n+1)}}{\partial\eta^2}+2\eta^3\frac{\partial\theta^{(n+1)}}{\partial\eta}-Prf^{(n)}\eta^2\frac{\partial\theta^{(n+1)}}{\partial\eta}. \tag{3.18}$$

It should be noted that other different choices of time differences are also possible. By means of the finite difference method we can obtain two linear equation system for $f_i^{(n+1)}$ and $\theta_i^{(n+1)}$ $i=(1,\ 2,....M)$ at the time step $(n+1)$, which can be solved, e.g. by the Guassian elimination.

3.4 Results and discussion

The system of non-linear partial differential equations consisting of Eqs. (2.14) and (3.14) with boundary conditions (3.15) and (3.16) has been solved numerically using finite difference scheme to compute the velocity and temperature profiles. The velocity field $f'(\eta)$ and the temperature profile $\theta(\eta)$ are plotted to analyzed the influence of the various parameters, for example, the viscoelastic parameter K, the suction parameter γ, the non-dimentional relative amplitude of frequency to stretching rate S, the magnetite parameter M and the Prandtl number Pr for the time series of the first five periods $\tau\in[0,10\pi]$ and the transverse profiles. Furthermore, we compute and show the values of the skin friction coefficient $Re_x^{1/2}C_f$ and the local Nusselt number $Re_x^{-1/2}Nu_x$ for different involving parameters both graphically and in tabular form.

Fig. 3.2 shows the time series of the velocity component f' at the four different values of distance y from the oscillatory sheet for the first five periods $\tau\in[0,10\pi]$ by keeping $S=2$, $M=10$, $\gamma=0.5$ and $K=0.1$, 0.4 fixed, respectively. It is evident from Fig. 3.2(a) $(K=0.1)$ that as we increase the distance from the oscillatory sheet, the amplitude of flow decreases. It is further noted that far away from the surface, the amplitude of the flow motion is almost is almost vanished (approached to zero) for larger distance from the surface. We observe the similar phenomenon from Fig. 3.2 (b) for the value of $K=0.4$. However, for $K=0.4$ the amplitude of the flow motion is large as compare with $K=0.1$. This indicates as increased effective viscosity with the increase of the non-Newtonian parameter K. It is also observed that

the amplitude of the flow motion increases in the presence of the suction parameter ($\gamma = 0.5$) as compared with ($\gamma = 0$).

Fig. 3.3 illustrates the influence of the viscoelastic parameter K, the magnetic parameter M and the suction parameter γ on the time series of the velocity component f' at a fixed distance $y = 0.25$ from the sheet, respectively. Fig. 3.3(a) shows the effect of the viscoelastic parameter K on the time series of the velocity profile f' by keeping $S = 2$, $M = 10$ and $\gamma = 0.5$ fixed. From this Fig. we see that the amplitude of the flow motion increases by increasing the value of K due to the increased effective viscosity and a phase shift occurs which increases with the increase of K. Fig. 3.3(b) gives the effect of the magnetic parameter M on the time series of the velocity component f' with fixed values of $S = 2$, $\gamma = 0.5$ and $K = 0.1$. It is found from this Fig. that the amplitude of the flow motion is decreased with the increase of the magnetic field. This is because for the present analysis the magnetic force acts as a resistance to the flow. Fig. 3.3(c) shows the time series of the velocity field f' for the different values of the suction parameter γ with fixed values of $S = 2$, $M = 12$ and $K = 0.2$. It is evident from this Fig. that the amplitude of the flow motion increases for the large values of the suction parameter γ. It is also noted that a phase shift occurs which also increases with the increase of γ. Furthermore, it is also observed from this Fig. that only slight phase difference occurs among the time series for various values of M in comparison with those for different values of γ and K.

Fig. 3.4 depicts the variation of the viscoelastic parameter K on the transverse profile of the velocity f' for the different values of $\tau = 8.5\pi$, 9π, 9.5π and 10π in the fifth periods $\tau \in [8\pi, 10\pi]$ for which a period motion has been reached. It can be seen from Fig. 3.4(a) that at a time $\tau = 8.5\pi$, the velocity $f' \to 1$ at the sheet $y = 0$ equating the surface velocity and $f' \to 0$ far away from the surface. It is also found that at this point of time, there is no oscillation in the velocity profile and the velocity f' is an increasing function of the viscoelastic parameter K, i.e. by increasing the values of K the boundary layer becomes thickener. Fig. 3.4(b) presents the velocity component f' at time point $\tau = 9\pi$ for various values of K. It can be seen from this Fig. that at this time point velocity profile f' is zero at the sheet $y = 0$ and far away from the wall it again approaches to zero. It is also observed that near the surface, there exist some oscillation in the velocity field and the amplitude of the flow is increased with an increase in K. This oscillation in the transverse profile is an evidence of a phase shift in the viscoelastic

fluid ($K \neq 0$) against the viscous fluid ($K = 0$). Fig. 3.4(c)-(d) displays the velocity field f' for others two time points within the fifth periods. It is evdient from Fig. 3.4(c)-(d) that the flow in the whole flow domain is almost in phase with the sheet oscillator in the case of Newtonian fluid ($K = 0$), as shown from the solid lines displayed in Fig. 3.4(a)-(d). Furthermore, we can see from Fig. 3.4 that the boundary layer thickness is increased by increasing the value of K.

Fig. 3.5 gives the effect of the magnetic parameter M on the transverse profile of the velocity component f' for the different times of $\tau = 8.5\pi$, 9π, 9.5π and 10π with fixed values of $S = 1$, $\gamma = 0.5$ and $K = 0.2$. It is evdient from this Fig. that the influence of the magnetic field causes to reduce the velocity field f' and the boundary layer thickness. As expected, this is because the magnetic force is a resistance to the flow and reduces the magnitude of the velocity. However at $\tau = 9\pi$ (Fig. 3.5 $((b))$) and $\tau = 10\pi$ (Fig. 3.5 $((d))$), there exist still the oscillations in the transverse profiles near the wall, their amplitudes are fairly small. It is also noted that for different values of magnetic parameter M, the phase difference is almost invisible.

Fig. 3.6 presents the variation in the transverse profile of the velocity field f' for various values of the suction parameter γ at different times of $\tau = 8.5\pi$, 9π, 9.5π and 10π in the fifth period by keeping $S = 2$, $M = 12$ and $K = 0.1$ fixed. The change in the velocity f' for different values of γ at time $\tau = 8.5\pi$ at the sheet can be seen from Fig. 3.6(a). It is found that the velocity is equal to the surface velocity ($f' = 1$) at the sheet $y = 0$ and far away from the sheet it approaches to zero. Furthermore, the velocity profile is increased by increasing the value of the suction parameter γ. The influence of the suction parameter γ on the velocity f' at the time $\tau = 9\pi$ is presented in Fig. 3.6(b). It is evident from this Fig. that at this time point the velocity takes its value at the wall almost to zero ($f' \to 0$) and a phase difference occurs as we increase the distance from the plate. It is also noted that a phase difference increases with the increase of γ. The velocity fields for other two time points within the fifth are plotted in Fig. 3.6(c) and (d) and the same observations are found.

Fig. 3.7 shows the effect of the viscoelastic parameter K, the magnetic parameter M and the suction parameter γ on the shear stress at the wall $Re_x^{1/2} C_f$ for the time series in the first five periods $\tau \in [0, 10\pi]$. Fig. 3.7(a) elucidates the change in the skin friction coefficients $Re_x^{1/2} C_f$ for different values of K by keeping $S = 5$, $M = 12$ and $\gamma = 0.5$ fixed. It is observed that the skin-friction coefficient varies also periodically due to the oscillation of the surface and

the amplitude of $Re_x^{1/2}C_f$ increases for large values of K. Fig. 3.7(b) gives the variation of the magnetic parameter M on the skin-friction coefficient $Re_x^{1/2}C_f$. It is evident from this Fig. that the oscillation amplitude of the skin-friction coefficient increases as M increases. Fig. 3.7(c) displays the results of the suction parameter γ on the skin-friction coefficient $Re_x^{1/2}C_f$ with fixed values of $S = 1$, $M = 12$ and $K = 0.1$. It is noted that the oscillation amplitude of the skin-friction coefficient $Re_x^{1/2}C_f$ is increased by increasing the values of suction parameter γ.

Fig. 3.8 displays the effect of the Prandtl number Pr, the suction parameter γ and the magnetic parameter M on the transverse profile of the temperature θ for the time point $\tau = 8\pi$ with fixed value of $S = 2$. Fig. 3.8(a) shows the variation of the transverse profile of the temperature distribution θ for different values of Pr at the time point $\tau = 8\pi$. As expected, it is evident from this Fig. that both the temperature distribution θ and the thermal boundary layer thickness are decreased for the large values of Pr due to the decreased thermal diffusivity. The influence of the suction parameter γ on the temperature field θ can be seen from Fig. 3.8(b) in the fixed time $\tau = 8\pi$. It is found that from Fig. 3.8(b) that the temperature is a decreasing function of the suction parameter γ. The thermal boundary layer thickness also decreases by increasing the value of γ. Fig. 3.8(c) gives the variation of the magnetic parameter M on the temperature profile θ for various values of M with fixed values of $S = 1$, $\gamma = 0.5$, $K = 0.2$, and $Pr = 5$. As magnetic parameter M increases, both temperature θ and thermal boundary layer thickness are increased.

Fig. 3.9 presents the results of varying the Prandtl number Pr and suction parameter γ on the time series of the temperature distribution θ in the first five periods $\tau \in [0,\ 10\pi]$ at a fixed distance $y = 0.25$ from the sheet. Fig. 3.9(a) shows the changes of temperature with respect to Pr by keeping $S = 2$, $\gamma = 0.1$, $K = 0.2$ and $M = 12$ fixed. It can be seen that with the increase of Prandtl number Pr, i.e., with decrease of thermal diffusivity or the increase of specific heat, the increase in the fluid temperature becomes slower. Fig. 3.9(b) illustrates the effects of the suction parameter γ on the temperature profile θ in the first five periods $\tau \in [0, 10\pi]$. It is noted from this Fig. that with the increase in the suction parameter γ , the decrease in temperature θ with time becomes slower. Furthermore, it is observed form Fig. 3.9, a small oscillation, which is superimposed on the monotonically increasing in temperature time series, can be identified for large values of Pr an γ.

Fig. 3.10 presents the physical significance of the Prandtl number Pr and the suction parameter γ on the time series of the local Nusselt number $Re_x^{-1/2}Nu_x$ in the first time periods $\tau \in [0, 10\pi]$. Fig. 3.10(a) depicts the influence of Pr on the local Nusselt number $Re_x^{-1/2}Nu_x$ with fixed values of $K = 0.1$, $S = 2$, $M = 12$ and $\gamma = 0.1$. One can see from Fig. 3.10(a) that the magnitude of the local Nusselt number $Re_x^{-1/2}Nu_x$ is increased by increasing the values of Pr. The variation of the suction parameter γ on the local Nusselt number $Re_x^{-1/2}Nu_x$ can be seen from Fig. 3.10(b). It is found that the local Nusselt number $Re_x^{-1/2}Nu_x$ has similar effects for the values of γ as compared with the case of Pr. However, it is noted from this Fig. that for $\tau = 0$, the local Nusselt number has its maximum and then decreases monotonically because for the given initial conditions, the temperature gradient at the sheet has its maximum initially and decreases with time.

Table 3.1 shows the numerical values of the skin friction coefficient $Re_x^{1/2}C_f$ for various values of S, K, M and γ at the different periods of time series $\tau = 1.5\pi$. It is evident from this table that the value of skin friction coefficient for the three different time periods $\tau = 1.5\pi$, $\tau = 5.5\pi$ and $\tau = 9.5\pi$ are almost identical. Furthermore, we can see that the periodic motion may be reached within the first period when the initial conditions are set up. However, the change of the skin friction coefficient from positive to negative by increasing the value of K indicates the large phase difference as K increases. It is also noted that the value of the skin friction coefficient $Re_x^{1/2}C_f$ are increased as the relative frequency to the stretching rate S, the magnitude M and the suction parameter γ are increased.

Table 3.2 gives the numerical values of the local Nusselt number $Re_x^{-1/2}Nu_x$ for various values of the Prandtl number Pr, the viscoelastic parameter K, the magnetic parameter M and the suction parameter γ at the four different times periods $\tau = 2\pi$, $\tau = 4\pi$, $\tau = 6\pi$ and $\tau = 8\pi$. It can be seen that the local Nusselt number increases by increasing the value of Pr,K, M and γ for all four times periods $\tau = 2\pi$, $\tau = 4\pi$, $\tau = 6\pi$ and $\tau = 8\pi$ and various values of local Nusselt number are also decreases when the time periods increases due to the decrease in the rate of heat transfer near the sheet.

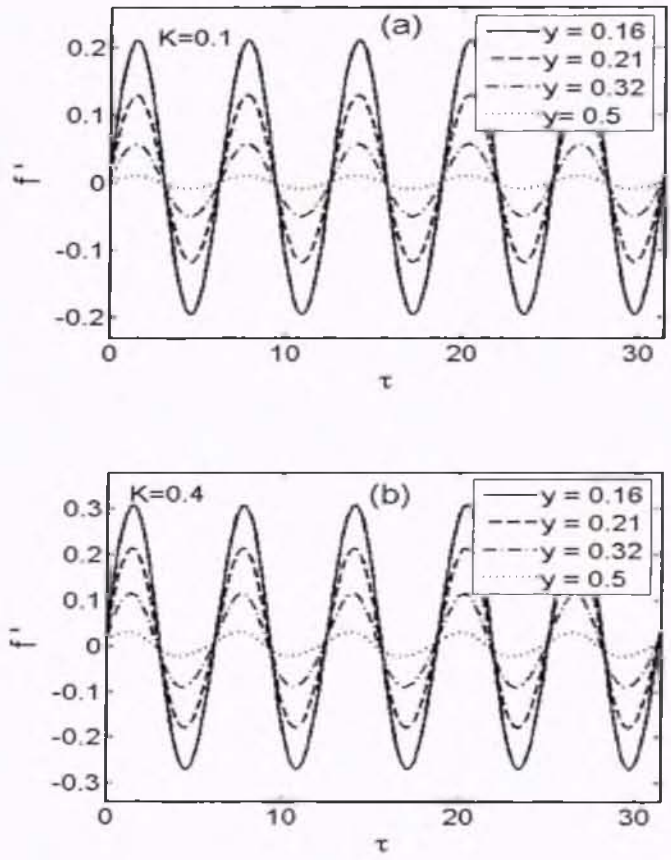

Fig 3.2: Time series of the flow of the velocity profile f' at the four different distances from the sheet for the time period $\tau \in [0, 10\pi]$ with $S = 2$, $M = 10$, $\gamma = 0.5$:(a) $K = 0.1$ and (b) $K = 0.4$.

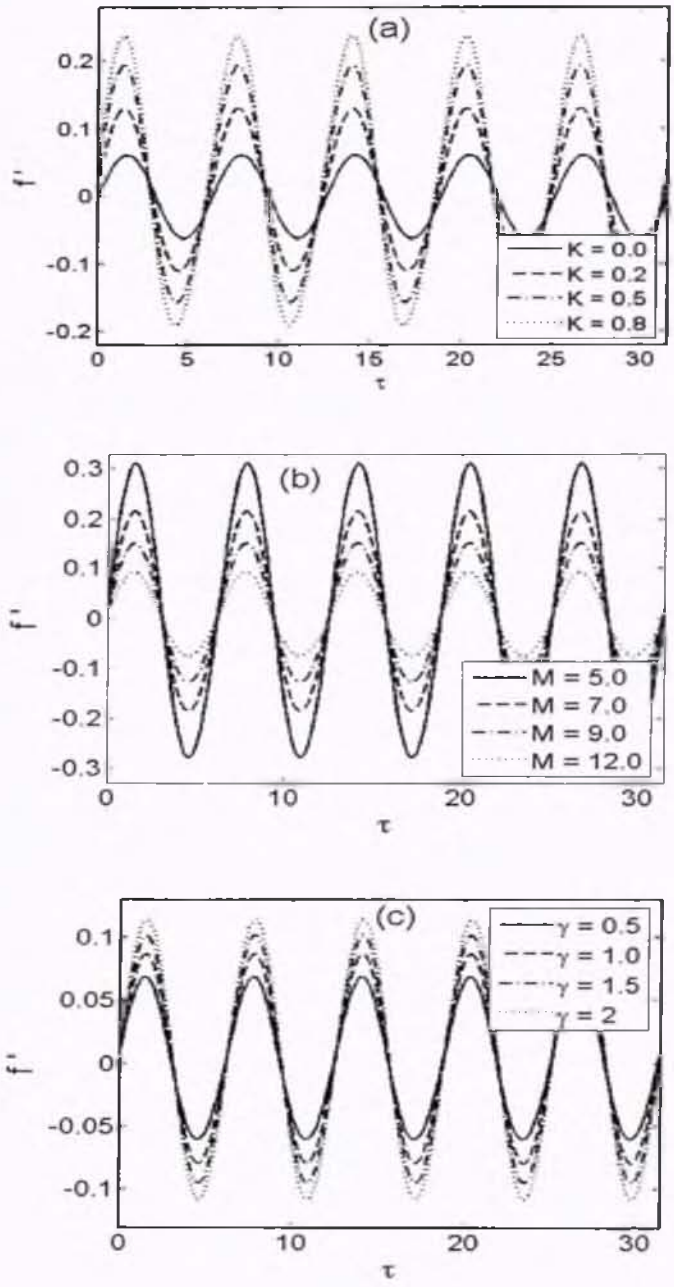

Fig. 3.3: Time series of the velocity profile f' in the first five periods $\tau \in [0, 10\pi]$ at a fixed distance to the sheet, $y = 0.25$: (a) effects of viscoelastic parameter K with , $S = 2$, $M = 10$, $\gamma = 0.5$, (b) effects of magnetic parameter M with $S = 2$, $K = 0.1$, $\gamma = 0.5$ and (c) effects of suction parameter γ with $S = 2$, $K = 0.1$, $M = 12$.

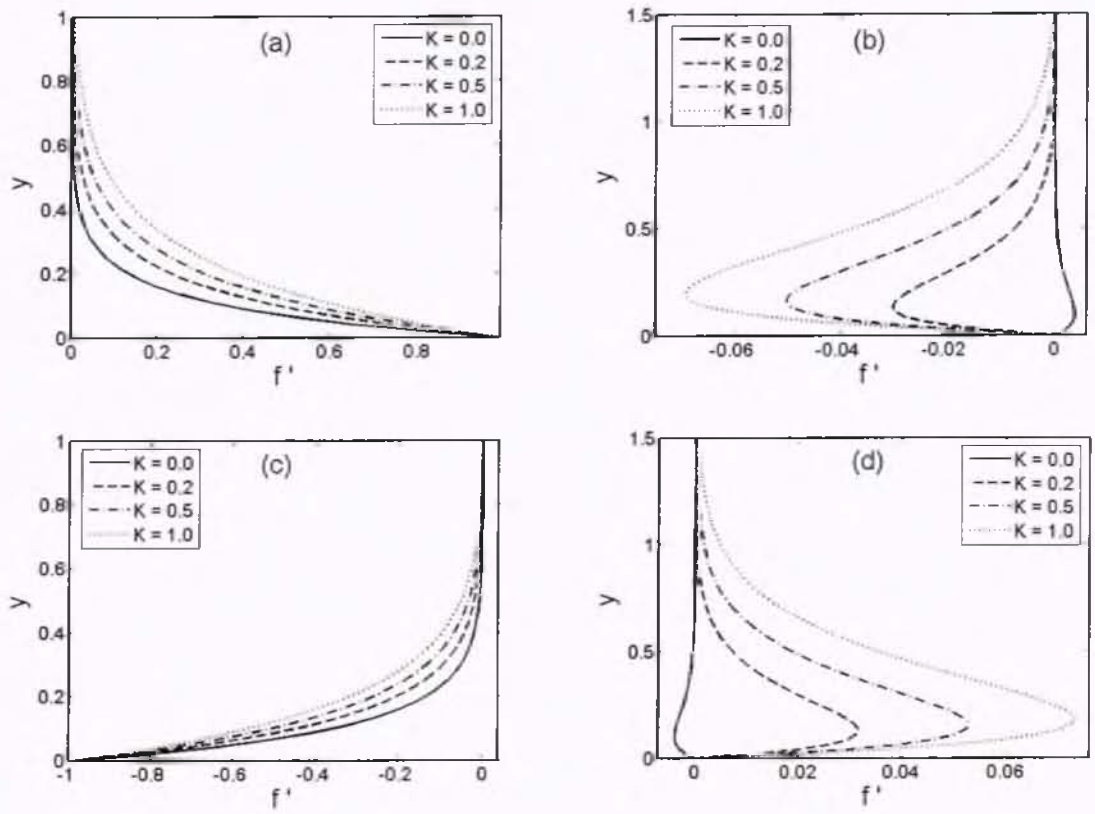

Fig. 3.4: Transverse profiles of the velocity field f' at the four different values of K for the fifth period $\tau \in [8\pi, 10\pi]$ for which a periodic velocity field has been reached: (a) $\tau = 8.5\pi$, (b) $\tau = 9\pi$, (c) $\tau = 9.5\pi$, and (d) $\tau = 10\pi$, with $S = 2$, $M = 10$ and $\gamma = 0.5$.

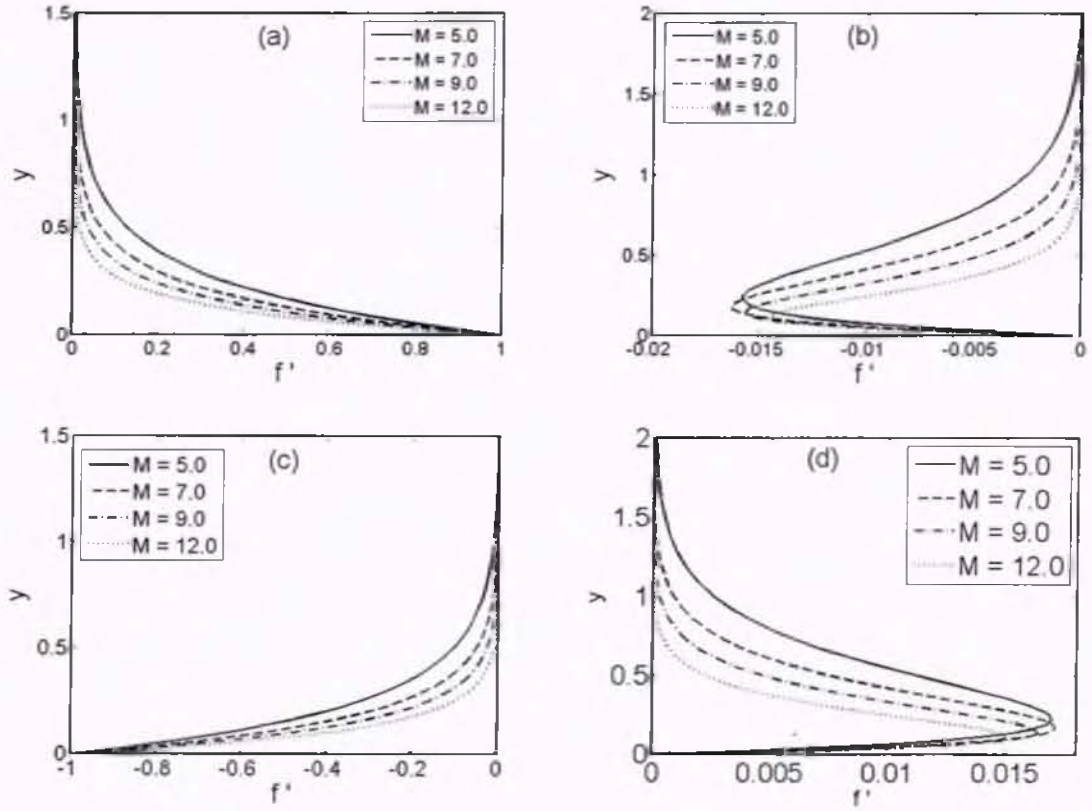

Fig. 3.5: Transverse profiles of the velocity field f' at the four different values of M for the fifth period $\tau \in [8\pi, 10\pi]$ for which a periodic velocity field has been reached(a) $\tau = 8.5\pi$, (b) $\tau = 9\pi$, (c) $\tau = 9.5\pi$ and (d) $\tau = 10\pi$ with $S = 1$, $K = 0.2$ and $\gamma = 0.5$.

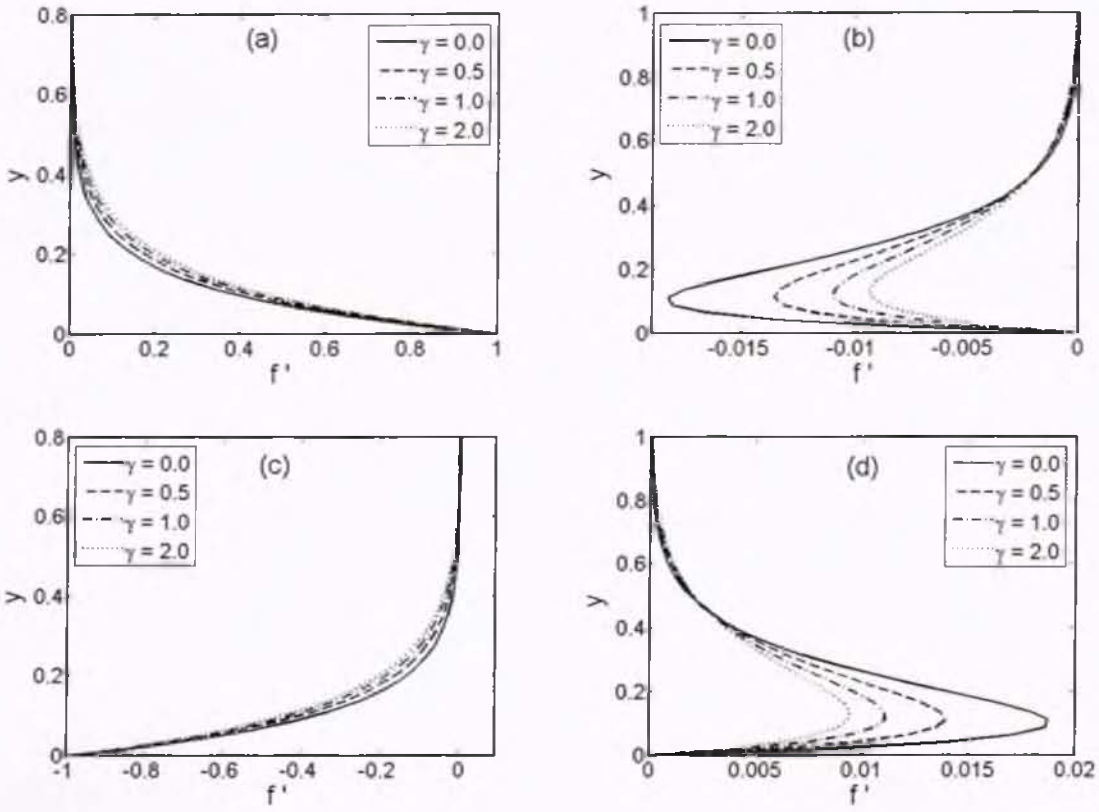

Fig. 3.6: Transverses profile of the velocity field f' at the four different values of γ for the fifth period $\tau \in [8\pi, 10\pi]$ for which a periodic velocity field has been reached: (a) $\tau = 8.5\pi$, (b) $\tau = 9\pi$, (c) $\tau = 9.5\pi$ and (d) $\tau = 10\pi$ with $S = 2$, $K = 0.1$ and $M = 12$.

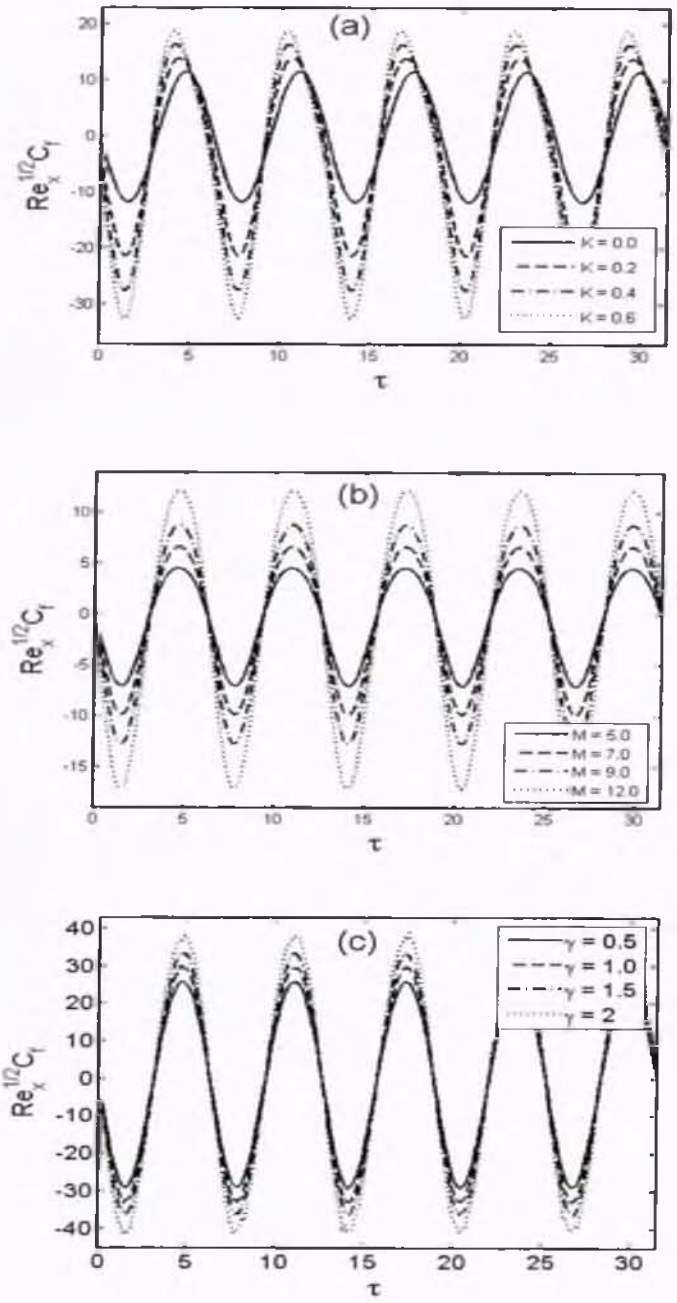

Fig. 3.7: Time series of the skin friction coefficient $Re_x^{1/2}C_f$ in the first five periods $\tau \in [8\pi, 10\pi]$: (a) effects of K with $S = 5$, $M = 12$, $\gamma = 0.5$, (b) effects of M with $K = 0.1$, $M = 12$, $\gamma = 0.5$ and (c) effects of γ with $K = 0.1$, $S = 1$, $M = 12$.

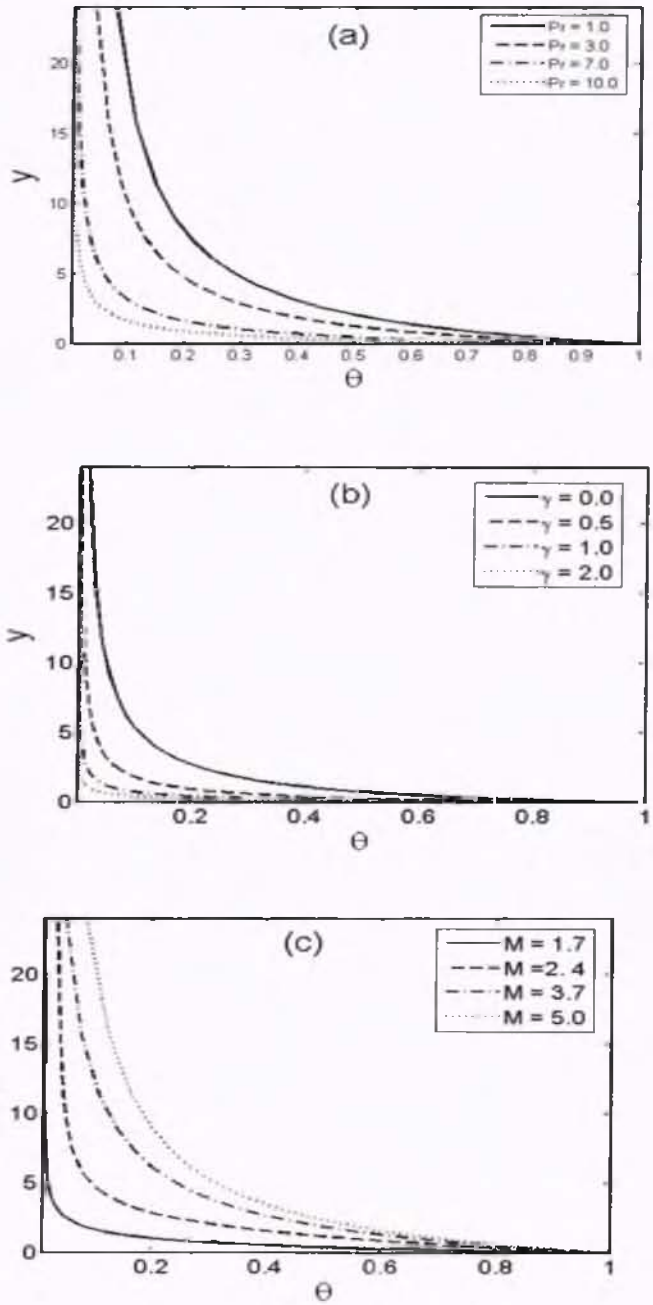

Fig. 3.8: Transverse profiles of the temperature field θ at the time point $\tau = 8\pi$: (a) effects of Pr with $K = 0.2$, $\gamma = 0.5$, $S = 2$, $M = 12$, (b) effects of γ with $K = 0.1$, $S = 2$, $M = 12$, $Pr = 5$ and (c) effects M with $K = 0.2$, $S = 1$, $\gamma = 0.5$, $Pr = 5$.

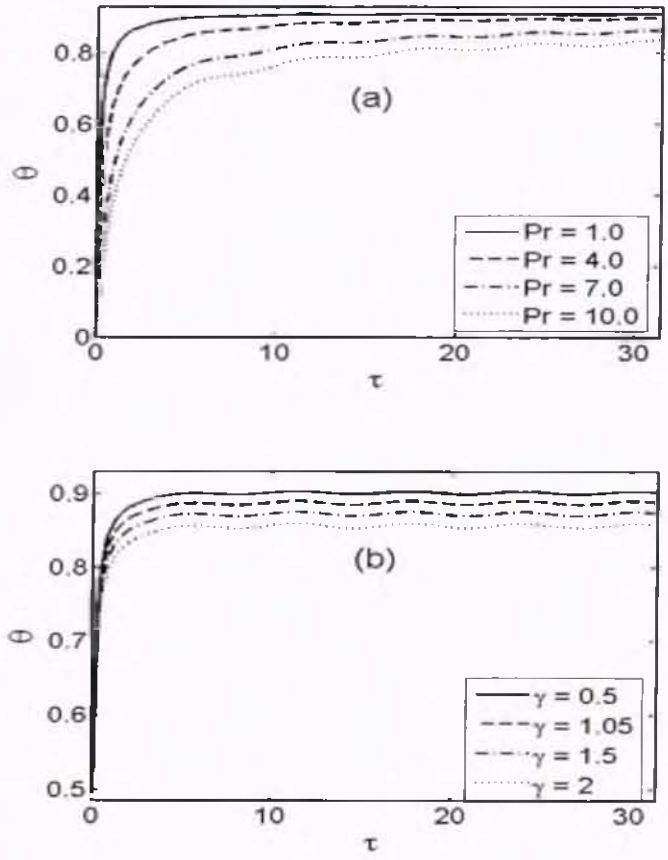

Fig. 3.9: Time series of the temperature profile θ in the first five periods $\tau \in [0, 10\pi]$ at a fixed distance to the sheet, $y = 0.25$: (a) effects of Pr with $K = 0.2$, $\gamma = 0.1$, $M = 12$, $S = 2$ and (b) effects of γ with $K = 0.1$, $S = 2$, $Pr = 0.5$, $M = 12$.

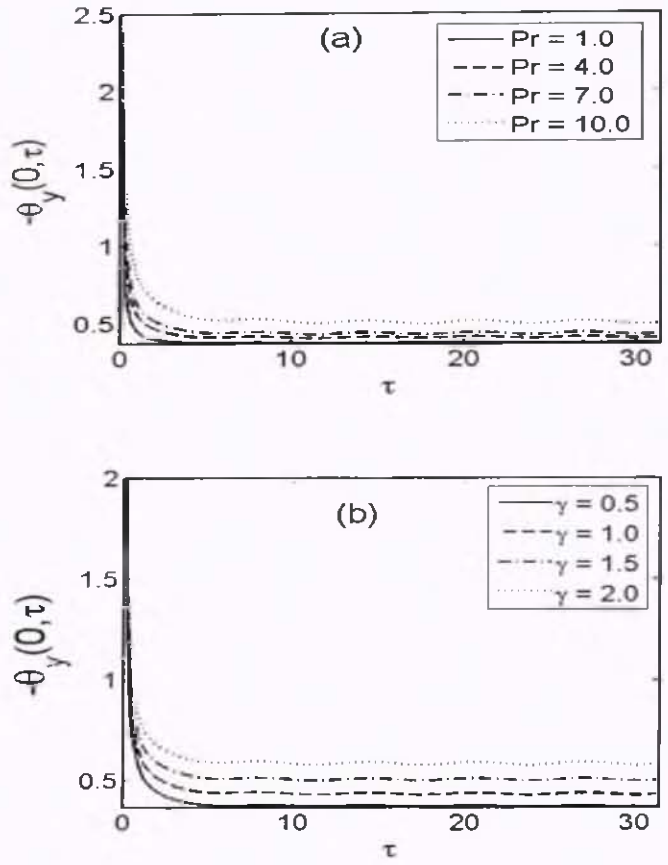

Fig. 3.10 : Time series of the local Nusselt number $Re_x^{-1/2}Nu_x$ in the first five periods $\tau \in [0, 10\pi]$: (a) effects of Pr with $K = 0.1$, $S = 2$, $M = 12$, $\gamma = 0.1$ and (b) effects of suction parameter γ with $K = 0.1$, $S = 2$, $M = 12$, $Pr = 0.5$.

Table 3.1: Numerical values of the skin-friction coefficient $Re_x^{1/2}C_f$ for different values of γ, M, S, K and three different time points $\tau = 1.5\pi$, 5.5π, and 9.5π.

S	K	M	γ	$\tau = 1.5\pi$	$\tau = 5.5\pi$	$\tau = 9.5\pi$
0.5	0.2	12	0.5	7.366961	7.366926	7.366853
1.0				7.476053	7.475794	7.476022
2.0				7.790178	7.789762	7.789836
3.0				8.202400	8.203105	8.202807
4.0				8.682439	8.682915	8.682859
1	0.0			11.724166	11.724170	11.724170
	0.2			7.476053	7.475794	7.476022
	0.5			1.630439	1.630612	1.630288
	0.8			-3.674101	-3.674865	-3.673871
	1.0			-6.956304	-6.956581	-6.955569
		5		2.732155	2.732089	2.7321590
		7		4.033675	4.0335629	4.0336795
		9		5.382074	5.382172	5.381872
		12		7.476053	7.475794	7.476022
		15		9.63356	9.633849	9.633961
		12	0.5	12.228457	12.224979	12.226006
			1.0	14.640233	14.6431046	14.646995
			1.5	16.605499	16.609908	16.5938511
			2.0	18.266957	18.250942	18.282542
			2.5	19.738842	19.764313	19.748855

Table 3.2: Numerical values of the local Nusselt number $Re_x^{-1/2}Nu_x$ for different values of Pr, K, M and four different points $\tau = 2\pi$, $\tau = 4\pi$, $\tau = 6\pi$, and $\tau = 8\pi$, when $S = 3$.

Pr	K	M	γ	2π	4π	6π	8π
1	0.2	10	0.1	3.955616	3.534056	3.419845	3.386686
3				6.137262	4.824050	4.346720	4.123851
5				8.179701	6.212831	5.439938	5.050552
7				6.137262	4.824050	4.346720	4.123851
10				8.179701	6.212831	5.439938	5.050552
1.0	0.0			3.926829	3.507357	3.393924	3.360903
	0.3			3.955694	3.534629	3.418675	3.385991
	0.8			3.974724	3.553044	3.433939	3.401853
	1.0			3.977727	3.556061	3.435827	3.4040001
	1.5			3.978796	3.557350	3.434803	3.403525
	0.2	7		4.603919	4.376667	4.315560	4.308688
		9		4.611656	4.329706	4.277972	4.274563
		12		4.628754	4.362667	4.299070	4.292905
		15		4.643919	4.376667	4.315560	4.308688
		20		4.663319	4.394577	4.336987	4.329227
		12	0.0	3.733978	3.324538	3.214515	3.182517
			0.5	4.965208	4.497219	4.366434	3.329196
			1.0	6.510785	5.995219	5.845916	5.804440
			1.5	8.392912	7.847680	7.684304	7.640581
			1.8	9.691076	9.138652	8.969649	8.925759

Bibliography

[1] B. C. Sakiadis, Boundary-layer behaviour on contious solid surfaces, AIChE J. 7 (1961) 26-28.

[2] B. C. Sakiadis, Boundary-layer behavior on continous solid surface: Boundary layer behaviar on continous flate surface, AIChE J. 7(1) (1921) 221-225.

[3] K. R. Rajagopal, T. Y. Na and A.S Gupta, Flow of a viscoelastic fluid over a streching sheet, Rheol. Acta. 31 (1984) 213-215.

[4] B. S. Dandapat and A. S. Gupta, Flow and heat transfer in a viscoelastic fluid over a streching sheet, Int. J. Nonlinear Mech. 24 (1989) 215-219

[5] J. B McLeod, K. R. Rajagopal, On the uniqueness of flow of a Navier-Strokes fluid due to a streching boundary, Arch. Rat.Mech. Anal. 98 (1987) 385-393.

[6] D. Rollins and K. Vajravelue, Heat transfer in a viscoelastic order fluid over a continuous streching surface, Acta Mech. 89 (1991) 167-178.

[7] R. Cortell, A note on flow and heat transfer of a viscoelastic fluid over a streching sheet, Int. J. Non-Linear Mech. 41 (2006) 78-85.

[8] R. Cortell, Flow and heat transfer of a electrically conducting fluid of second grade over a streching sheet subject to suction and to a transfer magnetic field, Int. J. Heat Mass Transfer 49 (2006) 1851-1865.

[9] R. Nazar, N. Amin, D.Filip and I.Pop, Stagnation point flow of a micropolar fluid twards a streching sheet, Int. J. Non-Linear Mech. 39 (2004) 1227-1235.

[10] A. Ishak, R. Nazar and I. Pop, Mixed convection stagnation point flow of a micropolar fluid twards a streching sheet, Mecccanica 43 (2008) 411-418.

[11] T Hayat, T Javed, Z Abbas, Slip flow and heat transfer of second grade fluid past a streching sheet through a porous space, Int. J. Heat Mass Transfer 51 (2008) 4528-4534.

[12] C.Y Wang, Nonlinear straming due to the oscillatory streching of a sheet of a sheet in a viscous fluid, Acta Mech. 72 (1988) 261-268.

[13] Z. Abbas, Y. Wang, T. Hayat M. Oberlack, Slip effects and heat transfer analysis in a viscous fluid over an oscillatory streching surface, Int. J. for Numerical Methods in fluid 59:443-458.

[14] Z. Abbas, Y. Wang, T. Hayat, M.Oberlack. Hydromagnetic flow in a viscoelastic fluid due to the oscillatory streching surface, Int. J. Non-Linear Mech. 43 (2008) 783-793..

[15] H. Schlichting, Boundary layer Theory, McGraw-Hill, New York,1964.

[16] J. E. Dunn and K. R. Rajagopal, Fluids of differential type: Critical review and thermodynamic analysis, Int, J. Eng. Sci.33 (1995) 689.